The inefficiency of "open-loop" fMRI experiments

David G. Norfleet

Thesis submitted to the Faculty of the
Virginia Polytechnic Institute and State University
in partial fulfillment of the requirements for the degree of

Master of Science
in
Biomedical Engineering

Stephen M. LaConte, Chair
Vincent M. Wang
Chris B. Arena

May 4th, 2023
Blacksburg, Virginia

Keywords: Default Mode Network, Event Related Functional Magnetic Resonance Imaging, Go/NoGo task, Human Connectome Project, Network State

The inefficiency of "open-loop" fMRI experiments

David G. Norfleet

ACADEMIC ABSTRACT

The default mode network (DMN) is a highly cited neural network whose functional roles are not well understood. Until recently, event related fMRI experiments used to study the DMN could only be conducted in an open-loop format. The purpose of this study was to demonstrate the potential statistical advantages of real-time fMRI studies to conduct closed-loop experiments to directly test putative DMN functions. Using both fMRI simulations and large archival datasets, we demonstrate that open-loop designs are less statistically powerful than closed-loop experiments that can trigger stimuli at controlled levels of brain activity. When simulating event scheduling on resting state data, DMN levels were normally distributed, but the event timing proved to be ineffective in capturing the highest and lowest DMN values on average across subjects. Statistical differences in DMN levels collected by the Human Connectome Project-Aging (HCP-A) during a Go/NoGo task were also reported, along with the network's distributional effects across subjects. When examining DMN levels in 136 subjects more prone to commission errors the mean DMN levels were reported to be higher during and prior to incorrect NoGo responses. Exploring DMN levels in these same individuals reacting to a Go task also revealed differing measurement patterns when compared to all 711 subjects in the study. Additionally, the distribution of total DMN levels across all participants, as well as during a Go or NoGo trial, showed a shift in the mean towards deactivation. Furthermore, the peak at this location was greater and revealed that increased sampling occurred at the mean and under sampling at the tails. Overall, the cumulative findings in this study were successful in providing statistical arguments to support propositions for more powerful closed-loop experimentation in fMRI.

The inefficiency of "open-loop" fMRI experiments

David G. Norfleet

GENERAL AUDIENCE ABSTRACT

Activity in a neural network is observed through the use of functional MRI (fMRI) by tracking higher levels of oxygenated blood to that region when active and lower quantities when inactive. Neural networks vary in their responsibilities, thus fMRI tasks are designed to trigger a response based on the functional role of the network. This can be exemplified by studying the blood flow to default mode network (DMN), a network responsible for mind wandering, during a task that requires focus. Researchers can then correlate moments of high activity, which indicates a greater degree of mind wandering, or low activity to a correct or incorrect response to the task. Unfortunately, the timing in which a task is presented to the participant is predetermined prior to the subject entering the MRI making it difficult to capture a correct or incorrect response at the precise moment of activation or deactivation. This concept is known as open-loop and often collects data at moments of neutral activity, neither high nor low. In contrast, a closed-loop design allows a researcher to monitor the DMN's activation levels in real time and present the task at a desired time. This provides more useful data to the experimenter as all recorded responses to the task correlate with exact moments of high and low activation. This makes claims about the neural network's role statistically more powerful as there is a greater quantity of data at these moments rather than during a neutral activation state. The purpose of this thesis is to provide statistical arguments that support propositions for more powerful closed-loop experimentation in fMRI.

This project is dedicated to all those who have loved and supported me during my time at grad school. To my parents, who have been there to celebrate my successes and provide comfort during my struggles. To both my siblings, who provided me with the confidence and determination to succeed, especially at the moments where that seemed impossible. To my girlfriend, who constantly encouraged and inspired me during the entirety of my thesis project. And to the countless friends I have made along the way. A special thank you to the young men of Smith Hall, Elon University, who I befriended in 2016 and who have been by my side ever since. I love you all.

Acknowledgments

I have had the privilege of encountering many incredible people during my years of schooling, both as a graduate student and an undergraduate. Firstly, thank you to my Principal Investigator, Dr. Stephen LaConte, for three incredible years your neuroimaging lab. I am so appreciative of your wisdom, patience, and guidance during my time as a member of the lab. The knowledge and skills that I have learned from you are truly invaluable. Thank you to Jonathan Lisinski for all your assistance during my thesis project. You took the time to meet with me every week during this process and were always there when I had a question or ran into obstacles. It is because of my work with you that I feel much more confident in my coding abilities in Matlab and performing data analysis. Thank you to both of my committee members, Dr. Vincent Wang and Dr. Christopher Arena, for your mentorship over the years. I was lucky to have both of you as professors during my undergraduate years and you have both played a role in molding me into the academic I am today. My growth and competency as a biomedical engineer is attested to the time and energy all these individuals invested towards my education. I acknowledge the impact all these individuals have had on my life and appreciate everything they have done for me.

Contents

List of Figures

List of Abbreviations

ACC Anterior Cingulate Cortex

AD Alzheimer's Disease

ADHD Attention Deficit/ Hyperactivity Disorder

BOLD Blood Oxygenation Level Dependent

CPT Continuous Performance Task

DMN Default Mode Network

DMPC Dorsal Medial Prefrontal Cortex

ER-fMRI Event Related Functional Magnetic Resonance Imaging

fMRI Functional Magnetic Resonance Imaging

HCP Human Connectome Project

HCP-A Human Connectome Project-Aging

IIVRT Intra-individual Variability of Reaction Time

MDD Major Depressive Disorder

PCC Posterior Cingulate Cortex

RIO Region of Interest

RT Reaction Time

SVR Support Vector Regression

VMPC Ventral Medial Prefrontal Cortex

WashU Washington University

Chapter 1

Background and Introduction

1.1 The Default Mode Network

The Default Mode Network (DMN) is a neural network reported to be responsible for mind wandering, autobiographical memory, and futuristic thinking [27]. It consists of the ventromedial prefrontal cortex (VMPC), dorsomedial prefrontal cortex (DMPC), and posterior cingulate cortex, which can be seen in Figure 1.1 [27]. The VMPC has shown to respond to aspects of one's personality, such as mood, while the DMPC and posterior cingulate cortex (PCC) correlate with personal judgment and past experiences [27]. Due to its regional makeup, task related fMRI studies have shown that the activity in the DMN decreases when participants are asked to focus on a task that requires a substantial amount of attention [2, 5, 10, 11, 19, 24, 27, 34]. During these studies the DMN is known to fluctuate between being highly activated, in correspondence with higher levels of daydreaming, and highly deactivated, correlative to higher levels of focus. While its activity can shift based on the state of mind the individual is in, the DMN is never fully deactivated [27].

Multiple studies have been carried out to examine the default mode network and its respected regions while performing a task or receiving a form of stimulus [2, 5, 8, 9, 10, 11, 17, 19, 24, 28, 34]. Although the methods for each case were different, correlative findings were made that could speak for the role the DMN plays in one's ability to pay attention. Much research

has presented that greater DMN activation or less DMN deactivation during or pre-task is linked to poorer results (i.e slower reaction times, errors occurring, etc.) [5, 10, 11, 19, 24, 34]. In contrast, Sadaghiani et al. reported that higher activity occurred in the DMN before a correct commission following an auditory stimulus [28]. Although these findings help present a greater understanding of the DMN, the open-loop experimentation process of finding correlations between task results and fMRI data after the fact is statistically inefficient. Moreover, by definition, the relationship between DMN and task performance are limited to correlative relationships. Additionally, this method makes for highly variable results regarding the timing of these findings. Esterman et al. utilized a pretrial window of 1.6 seconds that determined an increase in DMN activation preceded a commission error [11]. Boly et al. concluded that higher activity in the DMN 3 seconds before stimulation could predict poor results [5]. Weissman et al. reported that deactivation in task related regions 1.25 to 2.5 seconds before an event resulted in poorer results but failed to explore DMN activity prior to a lapse [34]. Similarly, Sadaghiani et al. showed that higher activity in the DMN 3 to 6 seconds before trials preceded better tasks [28]. These inconsistencies make it difficult to truly grasp how the default network behaves leading up to and following the delivery of a stimulus based on the independent timing methods and analysis strategies of the researcher.

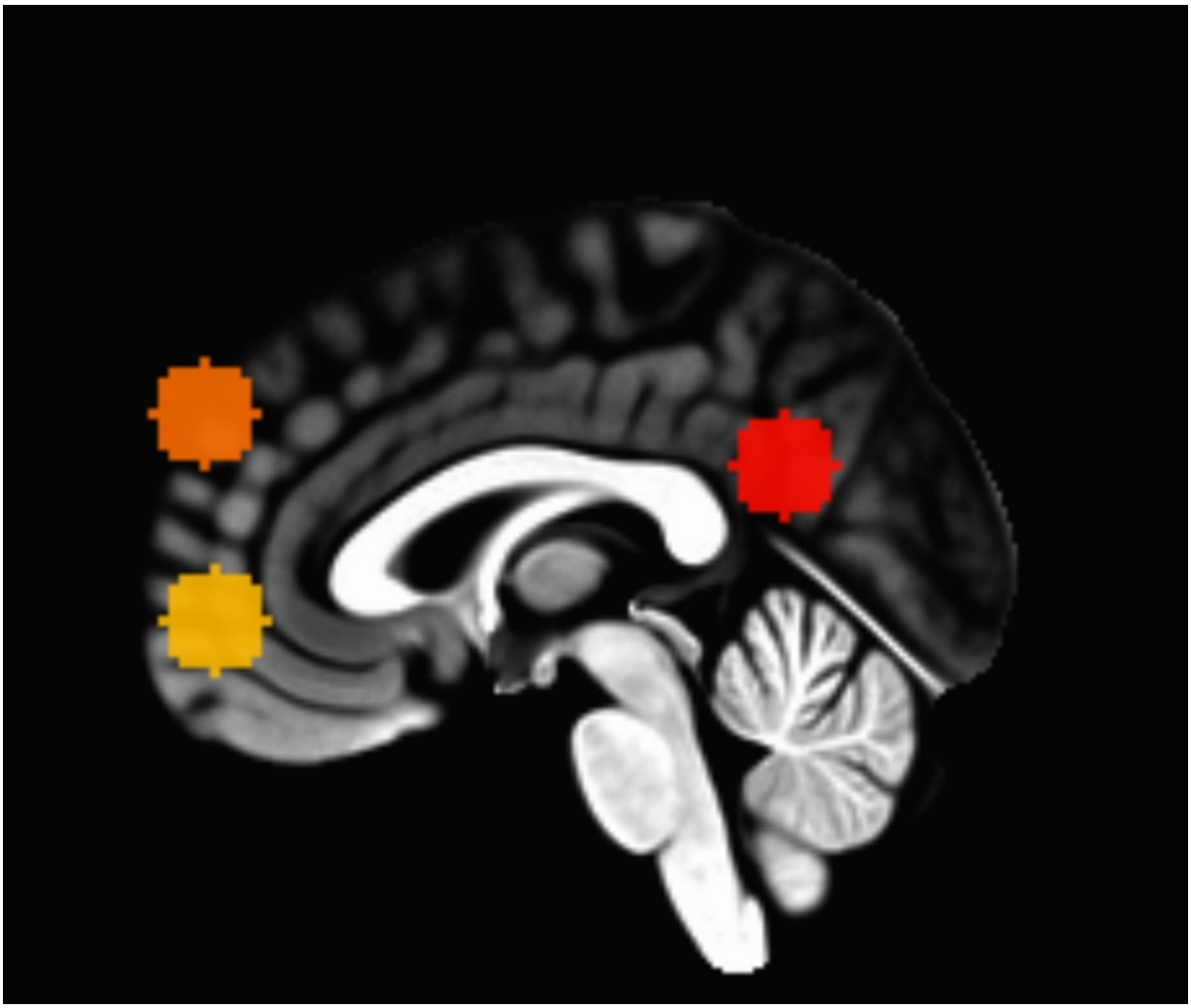

Figure 1.1: Sagittal view of the brain with DMN hubs highlighted. Yellow represents location of ventromedial prefrontal cortex, orange illustrates location of dorsomedial prefrontal cortex, and red identifies location of posterior cingulate cortex.

1.2 Functional Magnetic Resonance Imaging (fMRI)

Brain measurements are collected in the DMN through the use of event related functional magnetic resonance imaging (ER-fMRI) [22]. ER-fMRI allows researchers to track changes in the level of activity in a desired region through the use of blood oxygenation level dependent, or BOLD, signaling [22]. When a stimulus is presented, the activity level in the region of interest (ROI) increases and a larger volume of blood is presented to that area in a process known as the hemodynamic response [22]. This influx of blood changes the oxygenation level of the region and can provide a contrast for neural images as oxyhaemoglobin and deoxyhaemoglobin differ magnetically [22]. A baseline measure of the brain at rest is taken first to later compare with results from event related data [22]. This is performed because the brain is continuously active even while at rest [22]. Tasks are then designed to provoke a response in the region of interest based on its function [22]. The stimulus is often applied in a random, or "jittered", fashion in order to accurately capture its neural response and reduce habituation and expectation in the individuals [22]. Figure 1.2 demonstrates the general layout of a jittered event related task design. Utilizing a genetic algorithm or software application, the timing of the stimulus presentation will be given in the most optimal fashion [33]. A genetic algorithm works by creating heterogeneous designs based on the parameters set by the researcher and optimizes it based on measurement of fitness [33]. The models with the best fits can then have elements combined with one another to create an even more superior model [33]. This method can be made more statistically powerful by delivering more events in a rapid fashion, or rapid ER-fMRI exemplified in Figure 1.3, resulting in an increased number of samples collected at the end of the trial [22]. Furthermore, as the hemodynamic response has shown to be linear in nature, as seen in Figure 1.4, activity in the region can be estimated between samples [22]. DMN activation can be extracted from fMRI scans using a support vector regression (SVR) model [20]. Using resting state data to

train the model, an SVR model can then document the DMN activation that is recorded at each time point of a task scan [20].

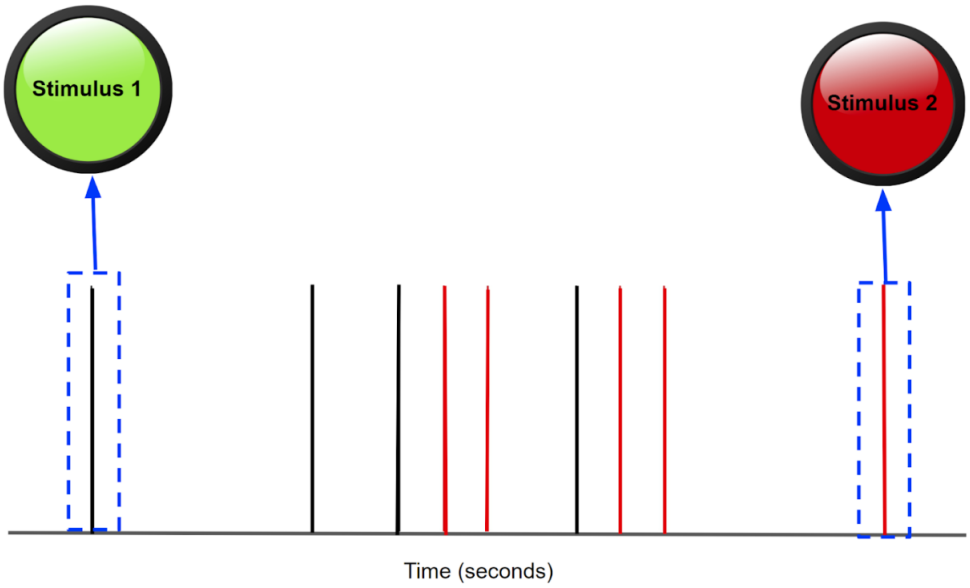

Figure 1.2: In an event related experiment, a number of events are presented at random throughout the duration of the trial. In this instance, the black vertical lines represent when stimulus 1 is presented and the red vertical lines represent the moments stimulus 2 occurred.

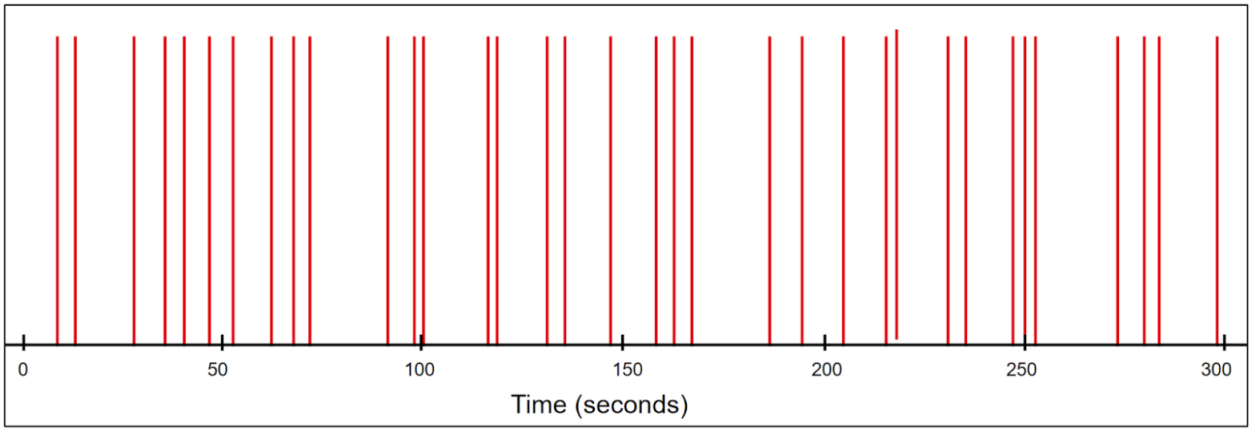

Figure 1.3: The red vertical lines represent when in time a stimulus is presented to the subject during a rapid event related fMRI study.

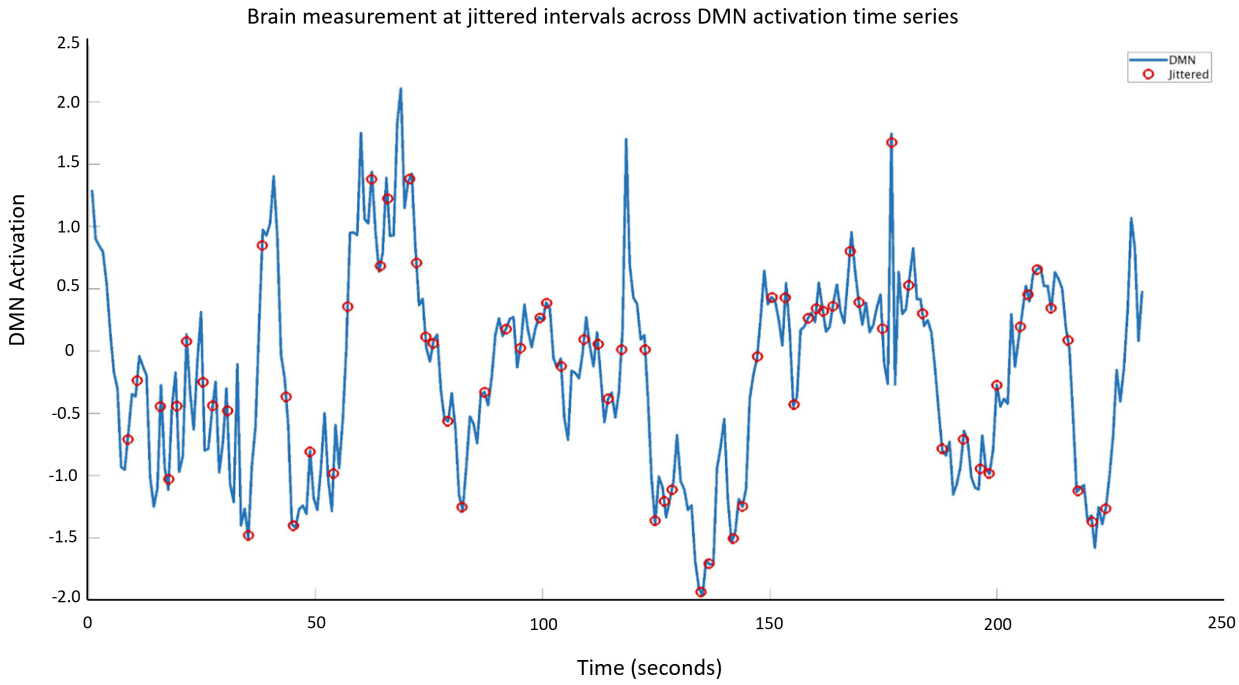

Figure 1.4: DMN activation over a given duration (blue line) and moments in time when a task is presented and brain level is collected (red dots). The DMN levels were measured every 800 milliseconds during this scan. Connections are able to be drawn between these instances to form the blue line due to the linear nature of the hemodynamic response.

1.3 Open-loop and Closed-loop

Many studies have made claims about the functional role of DMN based on examining task performance when the DMN is highly activated and highly deactivated [2, 5, 8, 9, 10, 11, 17, 19, 24, 28, 34]. The nature in which this data is collected and analyzed in literature is through an open-loop design process. Figures 1.5 and 1.6 show how an open-looped and closed-looped experiment are carried out. In an open-loop design, the presenter has chosen the most optimal time to deliver stimuli prior to the task being carried out, shown as the stimulus presentation of the red and green circles in Figure 1.5. The participant performs the tasks while fMRI measures DMN levels, and then data is analyzed after the fact making brain measurements an independent variable to stimulus protocol. Closed-loop designs work differently in that brain activity during the task is factored into the stimulus time and serves as a control signal for ongoing stimulus. Seen in Figure 1.6, stimulus is presented, brain measurement is taken, and ongoing brain signaling is tracked so that a new stimulus can be delivered again at a desired time based on activity levels.

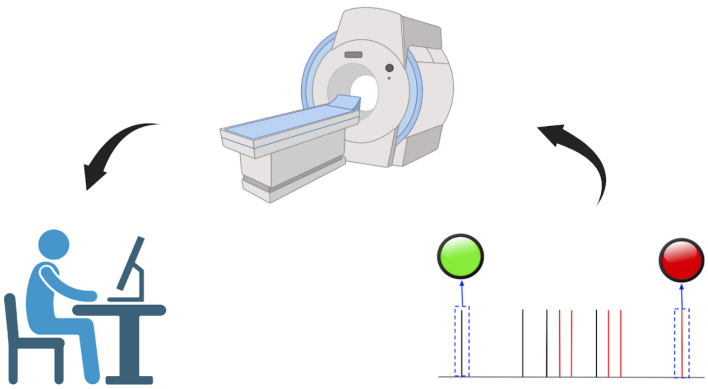

Figure 1.5: Open-loop design model. Optimal time for event presentation is chosen prior to scan (right), participants perform the task while MRI takes scans (middle), data is analyzed after experiment (left). Figure created with BioRender.com

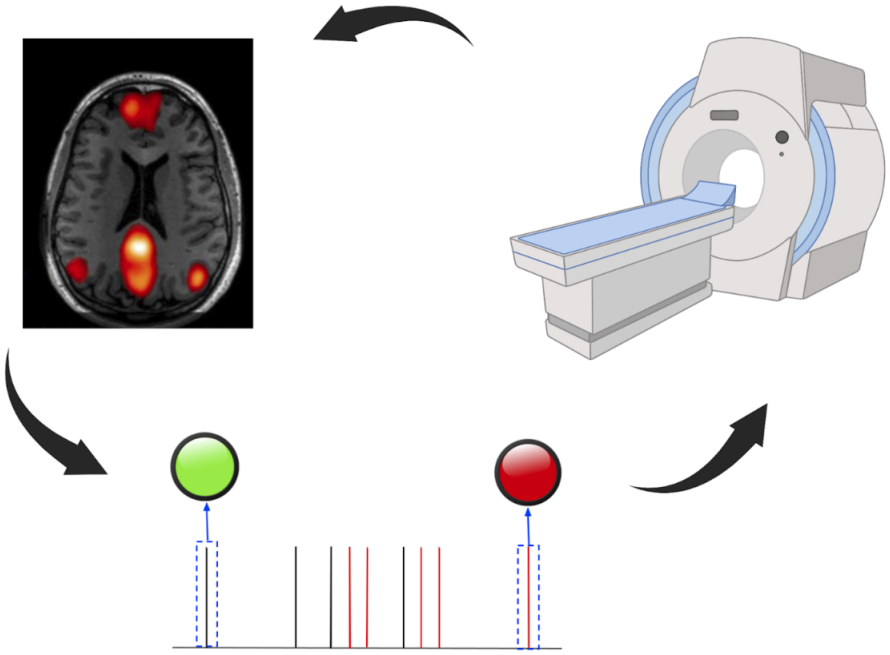

Figure 1.6: Closed-loop design model. Stimulus is presented to the individual (bottom middle), the participant performs the task and scans are taken (upper right), ongoing brain activity is monitored until a threshold level is recorded (upper left), new stimulus is presented and the process repeats. Figure created with BioRender.com

1.4 Human Connectome Project (HCP) and the Human Connectome Project-Aging (HCP-A) Study

Correlations between network activity and task performance can be generated from archived data, such as those collected from the Human Connectome Project and a Washington University study. A study involving the removal of motion artifacts from resting state scans was performed at Washington University [26]. 120 adults were asked to lay motionless with their eyes fixated on a white crosshair during the fMRI scan [26]. The NIH Human Connectome Project (HCP) began in 2009 and is a challenge shared amongst the science community that aims to better map neural networks in the human brain and their connections with one an-

other [1]. This is done through the identification of nodes that become active when a certain stimulus is presented to the subject in the MRI [32]. Various tasks have been used in order to target specific regions of the brain responsible for sensing, cognition, and processing [32]. Such tasks can be incorporated to study working memory, attention, emotion processing, language processing, and various other domains [4]. In order to study regions of the DMN, a variation of a Go/NoGo task was incorporated. Understanding these networks and their interactions provides greater insight into human behavior and can help explain thoughts and emotions [1]. Not only does this knowledge prove valuable in the perception of the mind, but allows for more productive research in all aspects of neuroscience, including treatments for disorders, illnesses, and injuries.

One particular study encapsulated within the HCP program is the Human Connectome Project- Aging (HCP-A). The HCP-A was created to provide an accessible dataset that showed the changes that occurred in the human brain as we age [6]. It involved over 1200 subjects ranging from 36 years old to greater than 100 years, with more than 600 of these participants returning for longitudinal assessments 20 to 24 months after the initial scan [6]. Subjects without any major diagnosed diseases were acquired through Washington University St. Louis, University of Minnesota, Massachusetts General Hospital, and the University of California [6]. Each participant was required to be in "typical health" for their age [6]. Age ranges were not uniform as there were 3 main cohorts: adults between 36 and 44, pre and peri menopausal women between the ages of 45 and 59, and older subjects between 80 and over 100 [6]. These groups aided in studying the brain in middle-aged adults, individuals in advanced years of age, and adults experiencing hormonal changes [6]. Each subject received scans while participating in a visuomotor task, an inhibitory control task, and a FaceName task, as well as during resting state [6]. During the visuomotor task, participants responded as quickly as possible by pressing one button when a red square appeared to the left of a central focal point and another button when it appeared to the right [6]. The inhibitory

control task was a Go/No-Go Conditioned Approach Response Inhibition Task (CARIT). Participants were required to respond as quickly as possible by pressing a button when a "Go" shape appeared or withholding from pressing the button when "No-Go" shapes appeared on screen [6]. The FaceName task had 3 sessions: a memorization phase, a distractor phase, and a recall phase [6]. Subjects memorized the names of respected faces shown on the screen and were asked to recall them after performing a "distractor" Go/No-Go task [6].

Chapter 2

Review of Literature

2.1 Go/NoGo Literature Review

An effective experiment utilized in DMN studies is the Go/NoGo task [3, 11, 16, 23, 25, 31]. During this task, subjects are required to press a button as fast as they can when a Go stimulus is presented and withhold a button press when a NoGo stimulus appears. Reaction times (RT) to button presses, and correct and incorrect responses to the appropriate stimuli are then collected. Oftentimes, correct commissions are regarded as a correct button press when a Go stimulus appears and incorrect commissions for when a button is pressed during a NoGo presentation. The task is purposefully designed to present more Go stimulus than NoGo in order to prime subjects to button pressing thus increasing the likelihood of an incorrect commission. Correlative findings are then made based on subjects' performance to the task and their DMN levels. Esterman et al. reported higher DMN activation prior to an incorrect commission and deactivation before a correct omission during their Go/NoGo experiment [11]. They additionally studied the variability in reaction time during the experiment and found greater DMN activity when variability was low compared to when variability was high [11]. RT variability to Go/NoGo trials and DMN activation levels have been examined across individuals who have difficulty focusing, such as those with ADHD [31]. In cases where subjects with ADHD were compared to a control when executing a Go/NoGo task, it was found that the intra-individual variability of reaction time (IIVRT) predicted from

variability in activity levels in DMN hubs differed between the two populations [31]. It was found that there was a higher IIVRT prediction in ADHD patients over the control group based on the variability in the hemodynamic response to correct rejections in the posterior cingulate cortex [31]. However, there was a lower IIVRT prediction in ADHD individuals over the control group based on the variability in the hemodynamic response to correct rejections in the precuneus [31]. This study compares to another conducted by Barber et al. in that they found that different hubs in the DMN respond differently to a Go/NoGo task [3, 31].

Barber et al. utilized two separate Go/NoGo trials titled "Simple" and "Repeat", the "Simple" task being a standard Go/NoGo trial and the "Repeat" requiring participants to remember the color of the screen from the previous run and respond if the next stimulus was a different color or abstain from responding if the color repeated itself [3]. The results showed greater suppression in the DMN occurred during trials with slower reaction times recorded and that negative RT-related activity peaked in the dorsal medial prefrontal cortex (dMPC) during the "Simple" tasks and in the ventral medial prefrontal cortex (vMPC) for the "Repeat tasks" [3]. Furthermore, while positive RT-activity, slower RT when activity increases, was mostly associated with "task positive" networks, there were a number of DMN voxels that responded positively during the Repeat trials [3]. As this was not the case for the Simple trials, it was shown that opposing RT responses in the DMN were the result of differing tasks, in that greater RT-related suppression was present in Simple tasks but greater positive RT-related activation occurred in Repeat tasks [3].

Go/NoGo experiments have been popular amongst studies related to major depressive disorder (MDD) [25]. In a literature review of fMRI studies interested in the impact of MDD, researchers compared 10 studies that utilized a Go/NoGo task and 1 that used a continuous performance task (CPT) [25]. They reported varying results related to DMN levels based on attention impairment caused by MDD but that activation patterns differed between healthy

controls compared to those with MDD, indicating cognitive impairment from this disease [25]. Two studies from the Piani et al. review compared anterior cingulate cortex (ACC) levels in MDD patients versus a control group during a Go/NoGo task [16, 23]. While the area of interest and the experiment were the same, they came to conflicting results. Korgaonkar et al. reported increased ACC levels in MDD subjects over control subjects during the Go/NoGo task [16], while the study by Nixon et al. found lower ACC levels in remitted MDD subjects compared to control subjects during the task [23]. Although the correlative findings between DMN levels and Go/NoGo performance differ, it has shown to be a reliable experimental method for triggering a DMN response in participants.

2.2 HCP-A Literature Review

Access to a large data set without the need to run an experiment has made the HCP-A study a valuable and inexpensive tool for studying ROIs, building models, and studying diseases and therapies [14, 15, 18, 29]. Gbadeyan et al. utilized the data from HCP-A, along with two other data sets, to build connectome- based predictive models for predicting response time variability within subjects [14]. It was the goal of this group to utilize these models as a way to determine cognitive ability in aging adults based on their response time variability in attention based tasks [14]. In comparison, MRI scans from HCP-A participants, in conjunction with scans from individuals with Alzheimer's disease (AD), aided in constructing machine learning models to identify early indicators of AD [18]. This group reported a 94% mean accuracy in recognizing AD and could determine individuals at higher risk of developing AD [18]. Arterial spin labeling data from the HCP-A was accessed in another study to observe white and gray matter differences in aging adults [15]. Sahib et al. applied the same Go/NoGo task as the HCP-A study in their experiments to better understand

the impact that ketamine infusion had on control networks in subjects suffering from major depression [29]. While this study did not employ the results from the HCP-A study, the use of their task helped identify BOLD activation decline in the DMN following each infusion [29]. This study concluded with ketamine therapy being acknowledged as an effective way in modifying certain neural networks which resulted in improving major depressive disorder [29]. Although not specified on studying the DMN, the data extracted from HCP-A or using its Go/NoGo task design has shown capable of making claims related to the network's activation levels [14, 29]. The volume of HCP-A, as well as its use of a task known to trigger a DMN response, makes it a promising data set to mine when investigating the DMN's role in performance to an attention based task.

2.3 Hypothesis and Purpose of Study

The high prominence in literature makes the DMN an advantageous network to research, however its functional role has not been narrowed down. This has been demonstrated by the highly variable correlative results revolving around the DMN's functional role during attention tasks [2, 5, 8, 9, 10, 11, 17, 19, 24, 28, 34]. It is proposed that performing real-time fMRI (rtfMRI) studies rather than an open-looped design model will remedy this. When stimuli are presented randomly in an open-loop method, collecting DMN data at desired levels becomes extremely difficult to do. Using a closed-loop design in fMRI will allow for greater control of when the DMN will be sampled, primarily, when it is highly activated and highly deactivated.

Closed-loop studies span the spectrum of modalities and facets of neuroscience such as neuromodulation and advancements in neural prosthetics [12, 21, 35, 36]. While rtfMRI is sometimes thought of as solely a technology for neurofeedback, the experimental flexibility

that this approach confers is vast and largely untapped. As a result, this has caused proposals being made for real-time fMRI but are less prominent [7, 13, 30].

The purpose of this investigation is to build statistical arguments for closed-loop studies in fMRI through the use of simulations, examination of Go/NoGo task data from the HCP-A and a simulated task performed on resting state data from a Washing University study. It is hypothesized that an open-looped fMRI simulation will be less efficient than its closed-loop counterpart. When investigating the DMN level distribution across participants, it is expected that there is an oversampling of DMN data around the mean when performing an open-looped experiment. Furthermore, it is anticipated that the distribution effects will differ between resting state DMN data and task data. It is also predicted that there will be significant differences between the DMN time series of individuals who answered correctly to NoGo tasks and those who performed this task incorrectly.

Chapter 3

Methods

3.1 Linear regression model

A data set of fictitious DMN responses was created using a normal distribution with a mean of 0 and standard deviation of 1. The data set was compiled into a 1000 x 1 matrix to mimic 1000 samples being collected by a "participant" in an ordinary fMRI experiment. Following the standard procedure of an open-looped experimental design, where the data is collected at random, jittered time intervals, 300 samples were randomly selected from the "participant's" data. This represented the x-values for the linear regression model and were assembled into a 300 x 1 matrix titled Ex1. Each point was assigned "noise" that was selected from a distribution normalized around 0 with a standard deviation of 3. This noise was then applied to a linear regression model, $y = 0.2x$, and compiled in a 300 x 1 matrix named Ey1. A linear trendline was calculated using the data in Ex1 and Ey1.

In opposition to this method of data collection, a closed-loop experiment was simulated by selecting 300 data points systematically for the "individual". The same data used for the random selection method was utilized and reconfigured in ascending order from lowest to highest. The "subject" obtained 300 data points consisting of their 100 lowest and 100 highest scores, located at the tails of their distribution, along with 100 middle scores. This was assembled into a 300 x 1 matrix titled Ex2. "Noise" was simulated in the same way as the random selection method and applied to the same regression model, $y = 0.2x$. A trend

line was also measured using this method. The accuracy of determining the real function, $y = 0.2x$, when using the two data collection methods was then examined.

3.2 Quadratic regression model

The same method for the linear regression model was used for the quadratic regression. In this case, the randomly selected values were placed in a matrix named Ex3 and the "tail sampled" data was compiled into the matrix Ex4. Ey3 and Ey4 were based on the regression function, $y = 0.2x^2 - 0.37x$, and represented the values for the random and "tail sampled" respectively. The accuracy of both methods was then examined by comparing the calculated function from its true form.

3.3 Variation calculation in regression models

Similar to the regression models predicted from the data of one "individual", the accuracy of these methods was examined across 100 "subjects". 1000 data points were selected from a normal distribution (μ=0, σ=1) 100 times to create a 1000 x 100 data matrix. 300 random samples were selected for each "participant" to form the x-values of the function, Exx1 (300 x 100). 300 samples of "noise" were simulated from 100 separate normal distributions (μ=0, σ=3) and were assigned to each row in the Exx1 matrix. The x-values and noise were integrated into the linear regression function, $y = 0.2x$, to form a 300 x 100 matrix, Exy1, and 100 trend lines were calculated based on these values. The mean and standard deviation of the slopes and y-intercepts for these trend lines were calculated.

The same methods were applied to the "tail sampled" selection method with the x-values assigned in the same way as the previous linear regression method. After the 1000 x 100

matrix was scaled smallest to largest, each of the 100 "participants" received 300 data points based on their individual highest, lowest, and middle results. This created the Exx2 matrix. "Noise" was applied and y-values were obtained in the same way as the random selection method to form Exy2 (300 x 100). Finally, each trend line was calculated and the mean and standard deviation measured. Each method's ability to accurately predict the slope of the linear regression model based on the data selected was gathered and assembled into a box and whisker plot. The confidence interval and margin of error of slope estimation, using 95% confidence, were calculated for both methods using the equations in Appendix A.

Box and whisker plots illustrating the variation in a and b values to the second degree polynomial were constructed using the same methods as the linear regression model. Data was extracted using the same processes and in the same quantities within 100 realizations, and noise was produced using the same methodology. In this case, the extracted x values and noise were applied to the $y = 0.2x^2 - 0.37x$ function. 100 trend lines were also predicted and the mean and standard deviation for the a and b values were found. These predictions were assembled into box and whisker plots, confidence intervals and margins of error were calculated.

The "participation" size was also changed when using both data selecting methods and the variation in slopes, confidence intervals, and margins of error were taken for each case. The precision of the random selection method was compared using population sizes ranging from 100 to 300 in increments of 50. For this simulation, 300 data points were collected from the tails of distributions from 100 "participants" and used to calculate the margin of error from the mean linear regression slope. 300 data points were then selected randomly to calculate the margin of error for the mean linear regression slope. This process of randomly sampling data and calculating the margin or error was repeated but with the population sizes increased to 150, 200, 250, and 300 participants. These calculations produced when randomly sampling data across various population sizes were compared to those calculated

when controlled sampling across 100 subjects.

3.4 Data from WashU study

3.4.1 Optseq2 and simulated task experiment

An event related scheduling software, optseq2, built a rapid event related fMRI design for each of the 120 adult participants from a Washington University (WashU) study [19]. Optseq2 created the timing sequence of event delivery for a theoretical experiment based on set parameters given to it. Optseq2 parameters contained in Appendix B. 130 resting state scans per subject were parsed from the WashU study and compiled into a Matlab matrix. The resting state scan duration was 0 to 325 seconds and was determined by multiplying the number of scans by the 2.5 seconds repetition time (TR) from the WashU study. Using this time course and the scans from each participant, DMN levels from 0 to 325 seconds were mapped in each individual. The time optseq2 chose to present Event 1 and Event 2 to each subject was determined and, using the WashU time course vector, DMN levels at each instance either event occurred could be estimated. The TR value used in the optseq2 parameters was 1.25 seconds and presented events at times not held within the DMN level time course domain. In order to estimate the DMN levels at these occurrences, linear interpolation between points was performed.

3.4.2 DMN distributions and statistical analysis of tails

DMN level distributions were created from every scan across all 120 subjects and from simulated task scans from every participant. The mean, standard deviation, kurtosis levels, and skewness of each distribution were measured.

In order to determine the degree of sampling at the tails of these distributions, 10 subjects were chosen at random and their maximum and minimum DMN levels were extracted from their resting state data and the data from both events. The mean and standard deviations for each circumstance's maximum and minimum values was calculated across the 10 individuals. This was repeated 5 times in total. The difference in mean highest and mean lowest DMN activation during rest and during the simulated task were graphed.

3.5 Data from HCP-A study

3.5.1 DMN extraction for NoGo task and Go task

Files regarding individual task performance in the HCP-A Go/NoGo task were parsed and loaded into Matlab along with each participant's DMN levels during the duration of the task. Participants' task performance was paired with their corresponding DMN measurements, resulting in 714 subject files. The time a stimulus was delivered to an individual was recorded along with the type of stimulus presented, a Go shape or NoGo shape, and their response, correct or incorrect, to that task. The reaction time to a Go stimulus was calculated by subtracting the time the image appeared on screen from the time the subject pressed their button.

290 DMN measurements were collected per individual. A DMN time course was plotted by multiplying the TR value for this experiment, 0.8 seconds, by the number of scans. This provided DMN levels based on time from 0.8 seconds to 232 seconds. Linear interpolation was used to predict the DMN level at the time a Go and NoGo stimulus was presented to each subject. The number of presentations for each trial differed between subjects. Across all subjects, the maximum number of Go stimuli presented to an individual was 92 and the

minimum number was 12, the maximum presentation of NoGo trials was 80 and the minimum was 0. DMN levels during a correct and incorrect response to a NoGo trial were found using the NoGo DMN measurement matrix and the reported responses from the HCP-A files.

Distributions were created showing every DMN measurement collected across each subject, every DMN measurement during Go trials, and all DMN levels during NoGo trials. 2 distributions were assembled to show the DMN levels based on a correct response or incorrect response to a NoGo trial. The mean, standard deviation, kurtosis level, and skewness for each distribution were found.

3.5.2 Participant age and mean DMN levels

Age varied within the HCP-A study; the youngest individual being 447 months old (∼37 years) and the oldest reported as 1200 months old (100 years). The mean DMN value for each subject was calculated along with their age and graphed in order to determine a trend between the two conditions.

Parsing through demographic information from each participant, it was determined that information was not provided for 8 of the 714 participants. Individual's over the age of 100 years old are also uncommon and HCP-A experimenters reported subject's that met this requirement as 1200 months to keep their identity secret from the public. In these instances the true age of the individual was not reported and all participants marked as being 1200 months old were excluded from this calculation. The number of participants used to identify a trend between age and mean DMN levels was 695. Linear regression function for this data was calculated along with the R-squared value.

3.5.3 DMN levels prior to stimulus presentation in NoGo studies

The DMN levels prior to a NoGo presentation were estimated. The range of time observed prior to a NoGo presentation spanned from 0.8 seconds to 7.2 seconds in increments of 0.8. Distinct matrices were assembled to separate the timing of a correct versus an incorrect NoGo response. Time domains prior to a correct and incorrect response to a NoGo trial were built by subtracting the 0.8 second increments from the time a NoGo stimulus was reported to have appeared. Using linear interpolation, the DMN levels at these new instances were calculated from each participant's separate DMN level time course.

Participants that answered at least 3 NoGo tasks incorrectly (n=136) were collected and their DMN levels prior to correct or incorrect response were separated from the rest of the 714 participants. Mean and standard deviations of DMN levels for both responses were reported in each individual. An overall mean and standard deviation for these average correct and incorrect values were then taken across all 136 participants. This method was repeated for the DMN levels reported prior to a correct or incorrect response. Standard error to the mean for the DMN levels reported for a correct or incorrect response during and prior to a NoGo presentation was calculated. In all, 10 mean DMN values were recorded in total, 1 during and 9 prior to, a correct or incorrect response each. A paired t-test was performed on correct and incorrect DMN levels in each of the 10 cases and Bonferroni correction accounted for. The age provided by 131 of the 136 participants that answered 3 or more NoGo trials incorrectly was reported to determine the impact of age on NoGo trial performance. The age distribution was plotted and mean and standard deviation found.

3.5.4 Distribution of resting state DMN and task DMN level

DMN levels for all 714 subjects during a resting state scan were extracted and the dataset reduced to 290 scans to match the number of task scans. Distributions of all DMN task levels and all DMN resting levels were compared and statistical analysis was performed.

3.5.5 Reaction time (RT) for Go trials

Reaction times for each participant's Go trials were collected. 3 subjects were excluded due to an error in recording the time they pressed a button resulting in a population size of 711. DMN levels to Go trials were collected based on 5 reaction time ranges ($RT \leq 0.2s$, $0.2s < RT \leq 0.4s$, $0.4s < RT \leq 0.6s$, $0.6 < RT \leq 0.8s$, $0.8 < RT$). DMN levels prior to these reaction speeds were determined similarly to finding DMN levels prior to a correct or incorrect NoGo trial. The time reported for each Go trial was subtracted by the same 10 intervals (0s to 7.2s) and linear interpolation was performed for each individual's DMN time courses. The DMN levels during and prior to the Go stimulus were then extracted and separated based on how fast the subject reacted. This allowed DMN levels to be tracked prior to Go presentations in each of the five RT intervals. The occurrences of each RT interval block are as followers: $RT \leq 0.2s$: n=12, $0.2s < RT \leq 0.4s$: n=5540, $0.4s < RT \leq 0.6s$: n=36245, $0.6 < RT \leq 0.8s$: n=6878, $0.8 < RT$: n=20. Mean DMN levels during and prior to each of these RT intervals were calculated along with the standard deviation and standard error of the mean.

This data for all 711 subjects was compared with the DMN levels based on reaction time in the individuals that answered at least 3 NoGo trials incorrectly. One subject was excluded from this data set as they were one of the three individuals who was removed prior, bringing the population size to 135. Mean DMN levels were calculated during and prior to a Go response in these 135 individuals in each of the five reaction time instances. The number of

instances each reaction time interval occurred in this population were as follows: RT$\leq$0.2s: n=7, 0.2s<RT$\leq$0.4s: n=575, 0.4s<RT$\leq$0.6s: n=4951, 0.6<RT$\leq$0.8s: n=2664, 0.8<RT: n=2. The values reported in the 711 individuals were compared with those found in the 135 participants.

Chapter 4

Results and Executive Summary of Results

Simulations revealed greater inefficiency in an open-loop experiment's capability to estimate the slopes of linear and quadratic functions. Closed-loop experiments produced lower variation and margins of error in their estimations. Event scheduling methods utilized by open-loop studies were incapable of extracting the highest and lowest DMN activation levels on average. Under sampling DMN levels at the tails was present in open-loop task distributions, as well as a shift in the mean towards the left. DMN values differed between correct or incorrect response to NoGo tasks during and before stimulus presentation. Differences in the DMN before correct and incorrect responses are most significantly different 2.4 seconds to 4.8 seconds before event occurrence. Mean DMN levels during Go trials differed between individuals prone to mistakes during NoGo trials and the entire subject population when comparing their reaction times. Mean DMN levels for these participants also showed variation in greater or lesser activation to the full population depending on the speed they responded to Go tasks.

4.1 Accuracy of regression models during one realization

The simulations of the linear regression model and the quadratic regression model both showed improved accuracy of predicting the actual function when sampling from the tails over sampling randomly from the distribution. Although the trend line calculated from "tail sampling" was shifted up due to the noise, it measured the slope of 0.2064. When the same data was randomly selected, it drew mostly from the center of the distribution and estimated a slope of 0.1245. This trend was repeated for the quadratic model with the random sampling being heavily focused around the mean of zero and drastically underestimating the function's a and b slope values, 0.047 and -0.288 respectively. When drawing data points from the tails, the estimation was greatly improved with an a value of 0.2066 and a b value of -0.3689.

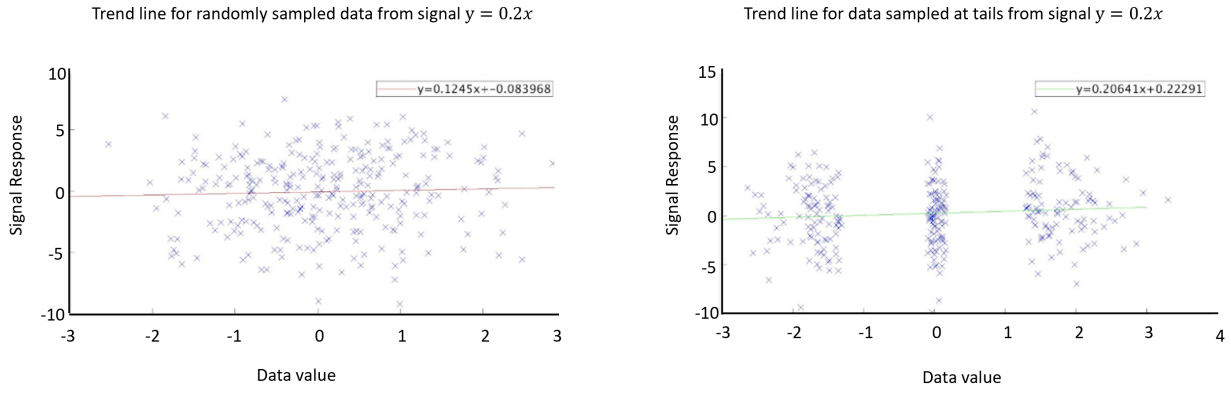

Figure 4.1: One realization depicting the accuracy of calculating the appropriate function, $y = 0.2x$, when selecting data at random (left) and when selecting data at the tail ends of a distribution (right).

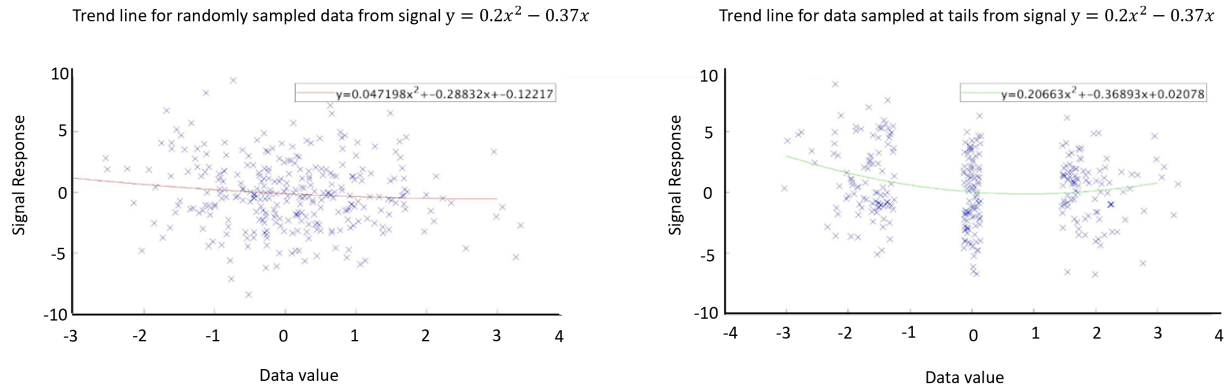

Figure 4.2: One realization depicting the accuracy of calculating the appropriate function, $y = 0.2x^2 - 0.37x$, when selecting data at random (left) and when selecting data at the tail ends of a distribution (right)

4.2 Variation of regression models over multiple realizations

The "tail sampled" method had smaller variations in the linear slope measurements for the 100 trend lines compared to the random data collection, illustrated by Figure 4.3. The distribution was much wider for the randomly selected data with a maximum slope of 0.6155 and a minimum value of -0.2435. This method also produced a mean slope value of 0.1842 (σ=0.1697) and an interquartile range of 0.2558. The distribution when sampling from the tails was much smaller with a maximum slope estimation of 0.4215, a minimum of -0.0614, a mean of 0.1926 (σ=0.0990), and an interquartile range of 0.1473.

The same pattern, depicted in Figures 4.4 and 4.5, was reported when using each method on 100 realizations to estimate the a and b values for the second degree polynomial $y = 0.2x^2 - 0.37x$. The distribution was wider for both variables when sampling data randomly over controlled sampling at the tails. A maximum value of 0.4633 and 0.0864 were reported for the estimated a and b values respectively when sampling at random. In comparison the maximum values for the variable when sampling at the tails was 0.4116 for variable a and -

0.0346 for variable b. The minimum values for the variable when comparing the two methods were (random: a= -0.1117 and b= -0.7589) and (tails: a= 0.0299 and b= -0.67.83). When data was collected at random the mean estimate for a and b were 0.2028 (σ=0.1286) and -0.3680 (σ=0.1805), respectively, with an interquartile range of 0.1788 for the a estimates and 0.2278 for the b estimates. The mean estimates for each variable were a=0.2038 (σ=0.0871) and b=-0.3903 (σ=0.1243) when data was collected at the tails. The interquartile range for variables a and b, respectively, were 0.1250 and 0.1576 using this method.

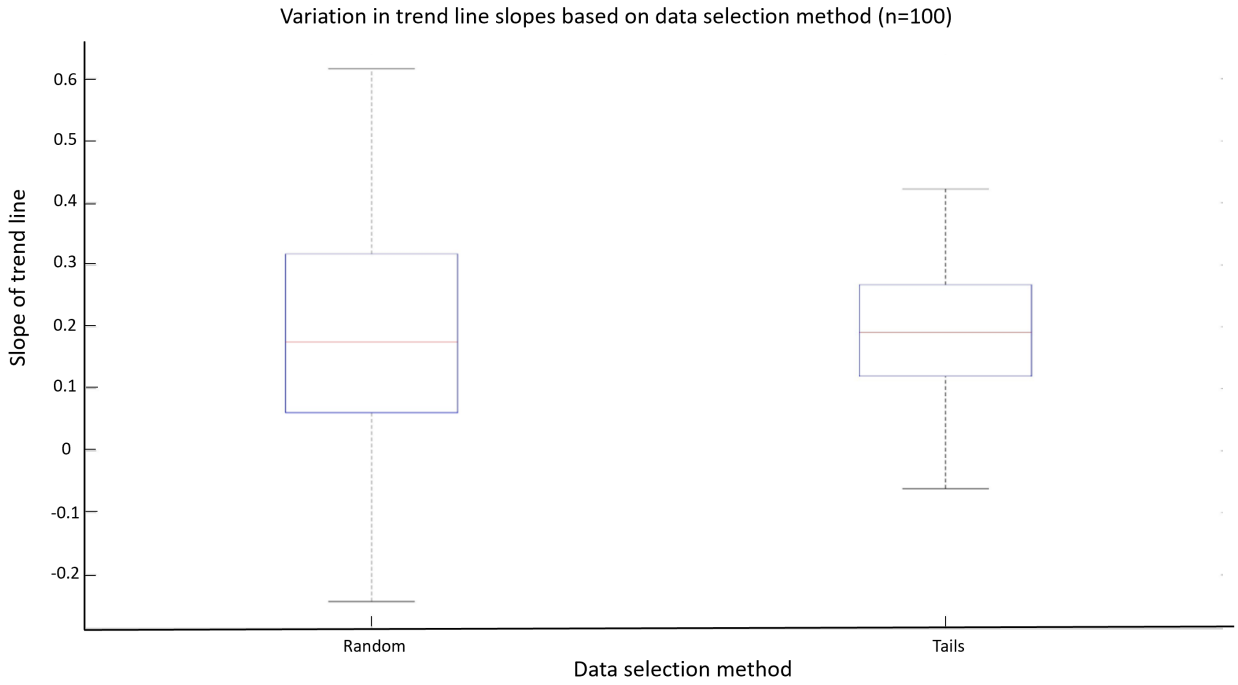

Figure 4.3: Variation in 100 linear trend line slopes obtained using data chosen at random (left) and data picked from the distribution tails (right).

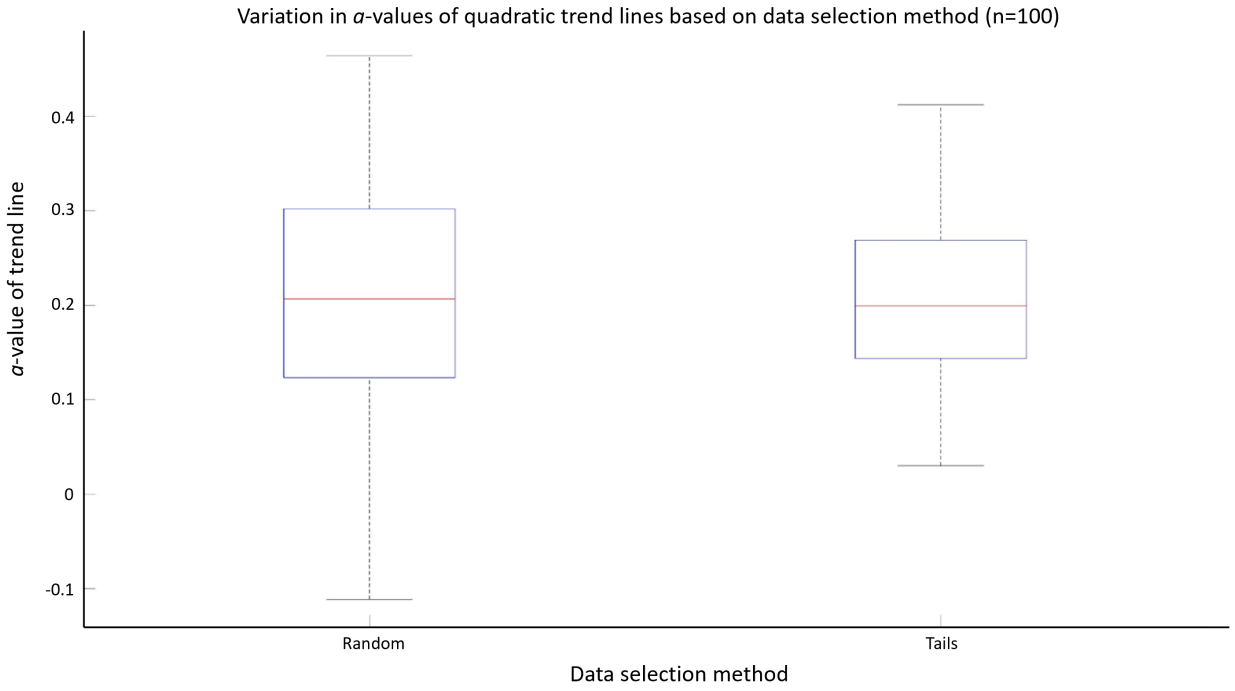

Figure 4.4: Variation in 100 a values to a second degree polynomial obtained using data chosen at random (left) and data picked from the distribution tails (right).

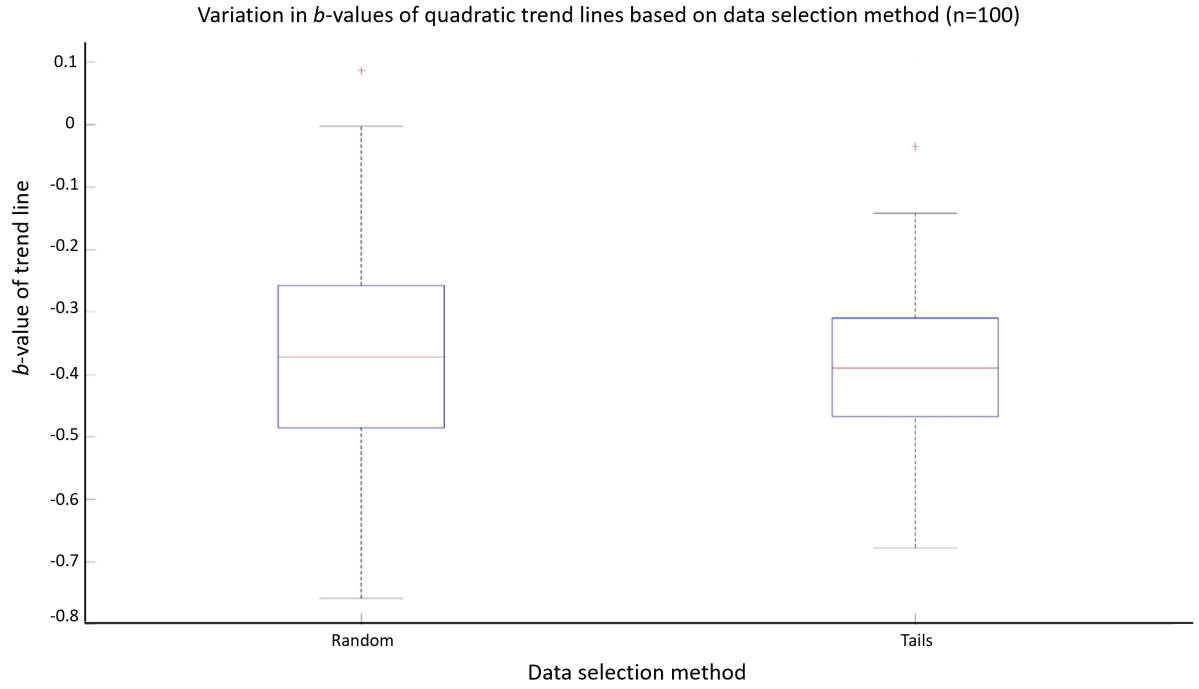

Figure 4.5: Variation in 100 b values to a second degree polynomial obtained using data chosen at random (left) and data picked from the distribution tails (right).

The confidence intervals of 95% confidence for the linear slope estimates were between 0.2175 and 0.1509 when sampling randomly and 0.2120 and 0.1732 when the data was sampled at the tails. The two simulations also produced margins of error of 0.0333 and 0.0194 for the random sampling and "tailed sampling" respectively.

The confidence interval for a value estimates when data is collected randomly was between 0.2280 and 0.1776 with a margin of error of 0.0252. 95% confidence produced a range between -0.3326 and -0.4034 in b value estimation using random sampling and a margin of error of 0.0354. When collected data at the tails, the confidence interval for a and b values was between 0.2209 and 0.1867 and between -0.3659 and -0.4147 respectively. Their margins of error being 0.0171 and 0.0244 explicitly.

The margins of error for linear slope estimation for both methods, shown in Figure 4.6, were found to be lower when sampling the data at the tails compared to when randomly sampling. Furthermore, the population size needed to exceed 200 subjects to bring the margin of error when randomly sampling below that of 100 subjects whose data was sampled at the tails.

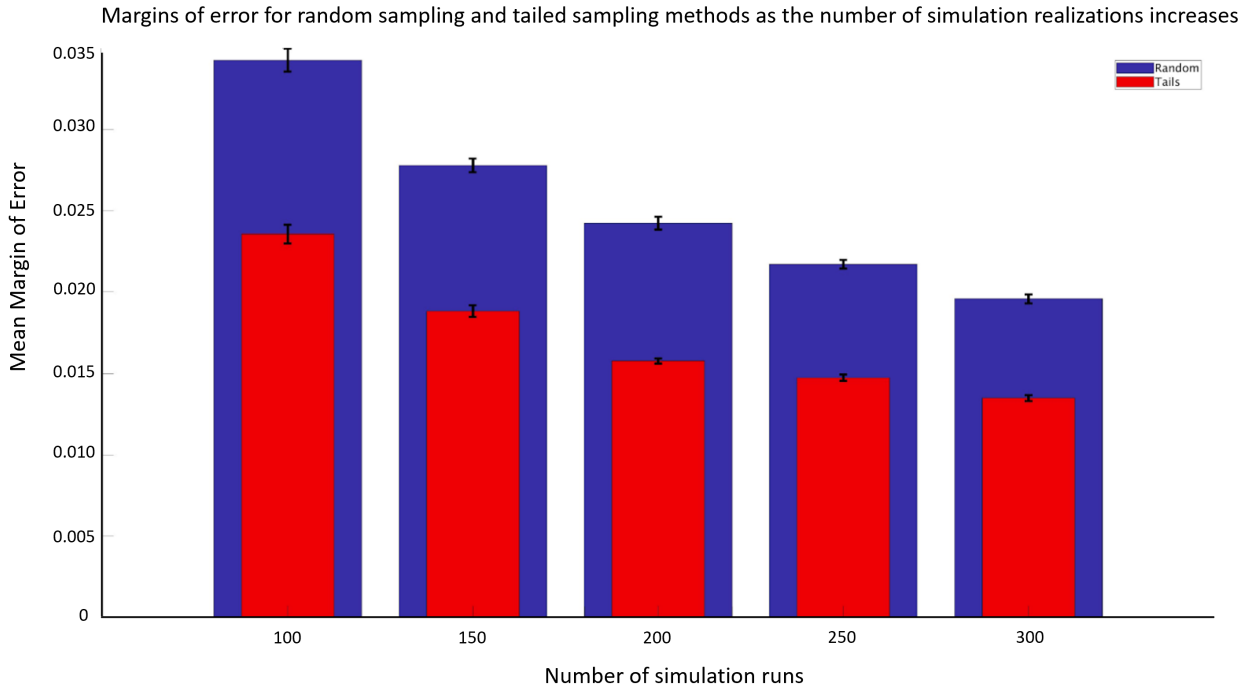

Figure 4.6: Margins of error for linear slope estimation using random sampling (violet) are compared to the margin of error for the tail method (red).

4.3 WashU task simulation distribution

The distributions created through the WashU data set were all standard normal. All DMN levels captured during scans, blue distribution in Figure 4.7, had a mean of 0.0045, standard deviation of 0.9985, kurtosis value of 3.0166, and skewness value of 0.0202. The DMN levels captured during the two simulated tasks followed the same pattern [(Event 1 (red distribution 4.7): μ=0.0158, σ=0.9512, κ=2.8611, γ=0.0255) (Event 2 (yellow distribution): μ=-0.0031, σ=0.9540, κ=3.0789, γ=-0.0109)]. All mean values were around 0 indicating no shifts towards DMN activation or deactivation during this simulation. The kurtosis value from Event 1 was slightly below 3, representing moderately lighter tails in this distribution when compared with the other two. Even still, kurtosis values were generally around 3, indicating an even collection of data and an avoidance of oversampling at the mean.

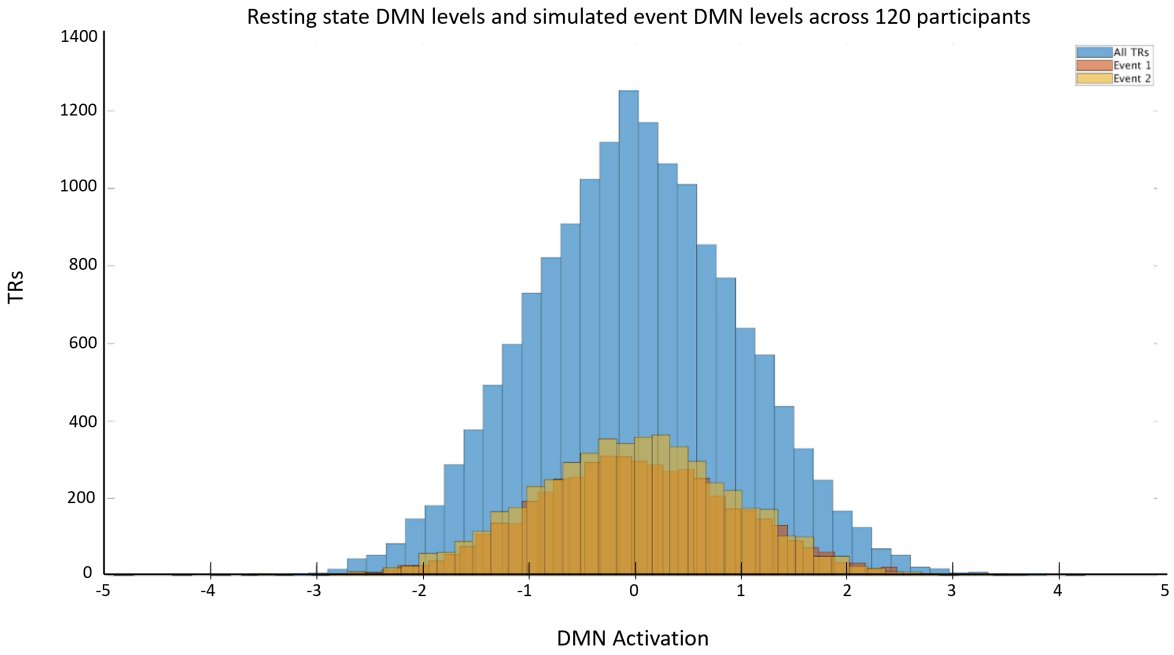

Figure 4.7: Distribution of DMN data from the WashU study. Blue represents every DMN scan collected, red describes all the DMN levels collected during Event 1, and yellow is the distribution of all the DMN levels collected during Event 2.

On average, task simulations were unable to capture DMN measurements far out on the tails, as seen in Figures 4.8 and 4.9. Performing a theoretical task study on resting state data failed to capture the DMN in its most activated and deactivated state. On average, the maximum and minimum DMN levels reported during both events were less than the possible measurements that could have been reported, as demonstrated by the blue bar in the figures (4.8, 4.9). The difference in magnitude across each iteration in the two figures does reveal a variation in the simulation's ability to capture highly interesting DMN values (i.e. very high and very low measurements). In some cases the mean values measured during an event were much closer to the levels that were collected across the entire scan. This phenomenon occurs at iteration 1 and iteration 2 for Event 1 shown in Figure 4.8, and again at iterations 4 and 5 for both Event 1 and Event 2 in Figure 4.9.

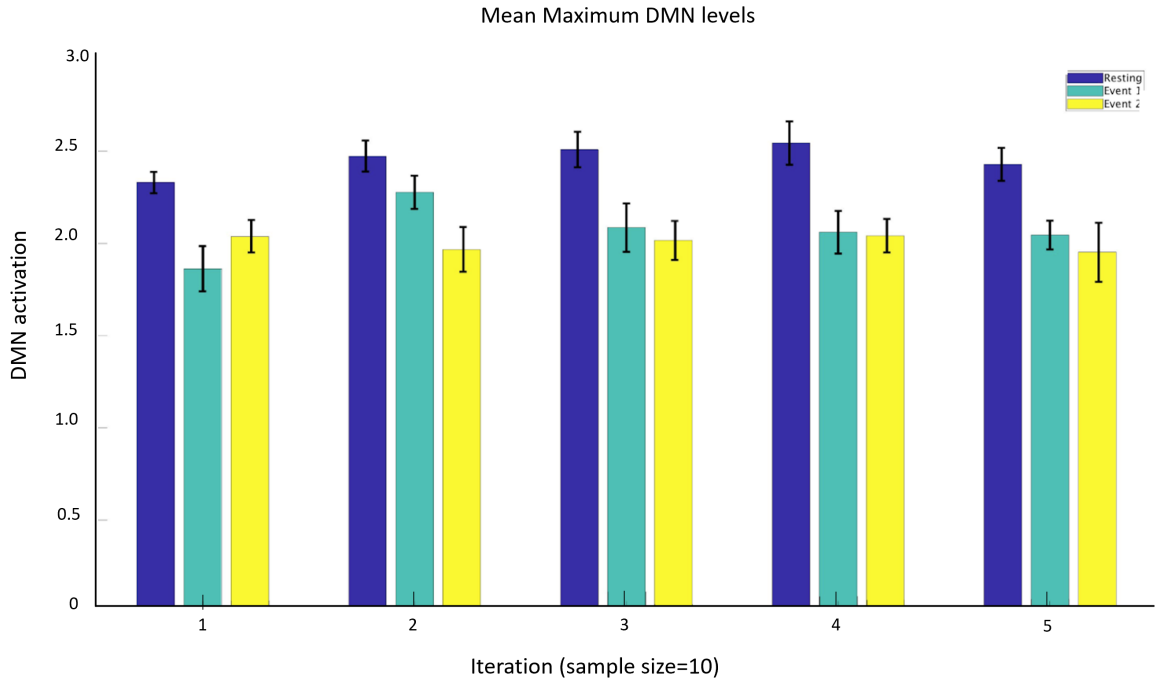

Figure 4.8: Mean maximum DMN levels from 5 iterations of testing. Each iteration randomly selected 10 individuals and had their maximum DMN levels extracted from all their possible scans (blue), during Event 1 (cyan), and during Event 2 (yellow). The mean maximum value was taken across the 10 individuals for all three cases.

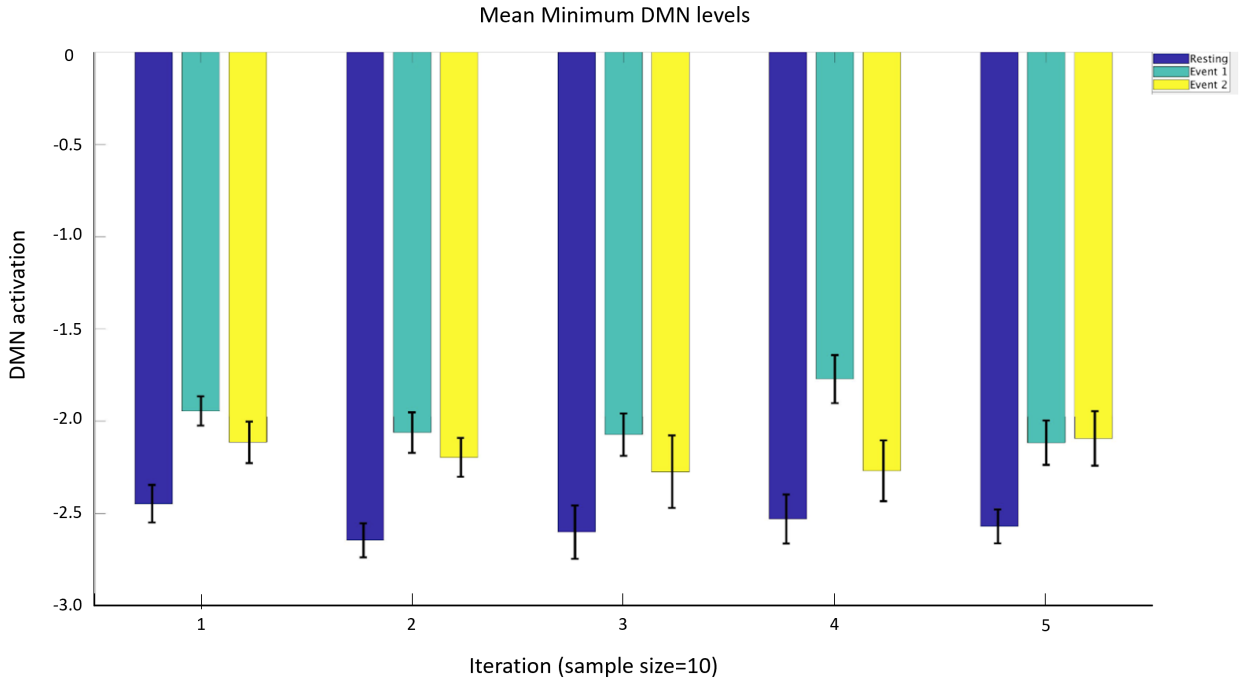

Figure 4.9: Mean minimum DMN levels from 5 iterations of testing. Each iteration randomly selected 10 individuals and had their minimum DMN levels extracted from all their possible scans (blue), during Event 1 (cyan), and during Event 2 (yellow). The mean minimum value was taken across the 10 individuals for all three cases.

4.4 HCP-A task data distributional effects

DMN levels collected during an event related task differed from the simulated task data from the WashU study. The distribution of measurements collected during the entirety of the task, shown in blue for Figure 4.10, had a mean value of -0.3962, a standard deviation of 0.8834, kurtosis level of 3.5002, and skewness of -0.0175. The data collected during Go trials and NoGo trials of the task exhibited a similar pattern [(Go (yellow distribution 4.10): μ=-0.4090, σ=0.8791, κ=3.5097, γ=-0.0128) (NoGo (orange-red distribution 4.10): μ=-0.4083, σ=0.8574, κ=3.4786, γ=-0.0338)]. Each instance was shifted towards a deactivated state as the means were moderately negative. In all three cases, the distributions do not hold normal tendencies as can be seen by their large peaks, high kurtosis values, and relatively lower standard deviations. These configurations show an excess of data sampled around the mean and under sampling of the tails.

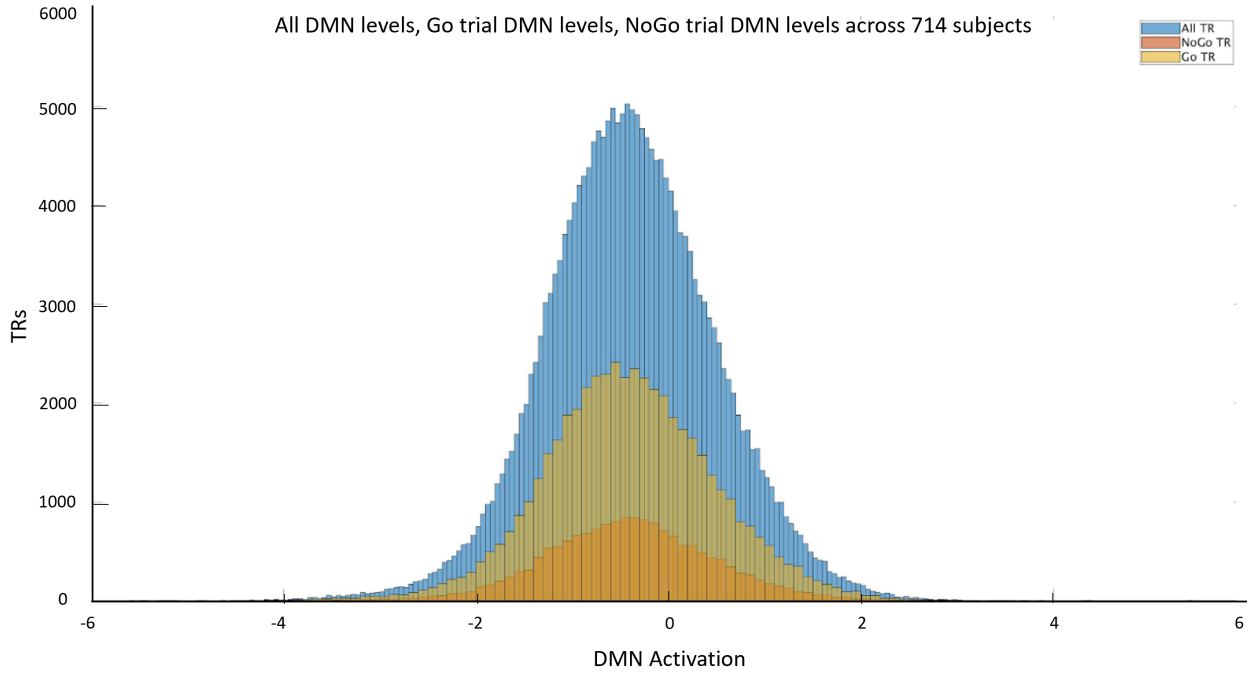

Figure 4.10: Distribution of DMN levels from 714 subjects undergoing a Go/NoGo task. All DMN measurements during time in MRI scanner (blue), DMN measurements during Go trials of task (yellow), DMN measurements during NoGo trials of task (orange-red).

There was a greater number of correct responses, depicted in the green histogram in Figure 4.11, than incorrect occurrences. The DMN distribution based on NoGo trial performance was similar to that of the DMN collected at every NoGo scan [(Correct (green distribution 4.11): μ=-0.4130, σ=0.8635, κ=3.4512, γ=-0.0219) (Incorrect (black distribution 4.11): μ=-0.3671, σ=0.8020, κ=3.7460, γ=-0.1386). Neither cases demonstrated any skewness but both showed a left shift with a negative mean value. Both distributions express outliers in the tails, this especially being the case for incorrect responses indicated by the larger kurtosis value. Both distributions express higher peaks at their mean, affirming a tendency for data to be collected around that value.

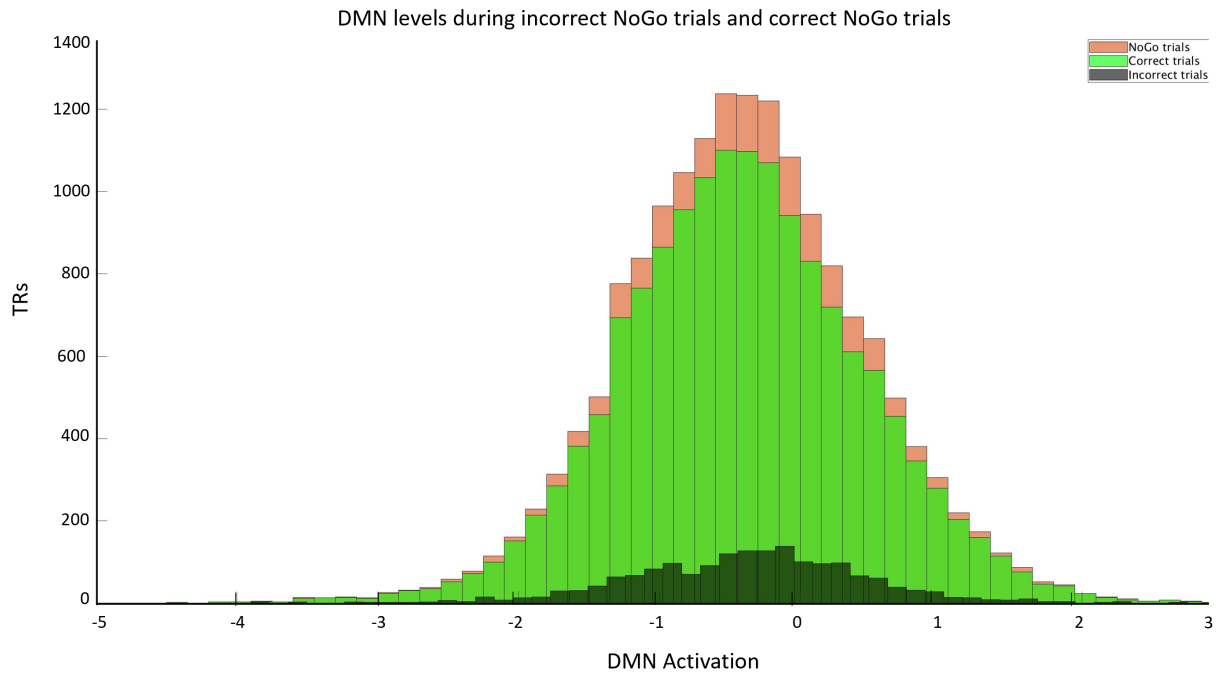

Figure 4.11: Distribution of DMN levels from 714 subjects undergoing NoGo trials. All DMN levels collected during Go/NoGo task (orange), DMN measurements during a correct response (green) and DMN measurements during an incorrect response (black).

4.5 Age and mean DMN levels in participants

Linear regression between individual's age and their mean DMN measurement during the task produced a function of $y = 0.00038494x - 0.67069$ (p-value intercept: 3.2467e-9, p-value slope: 0.011364), depicted in Figure 4.12. The accompanying R-squared value to this function was 0.00921. The coefficients of the model describe significance at -0.67069 with small divergence due to a minute slope value. This model does not reveal any relationship between one's mean DMN levels based on their age.

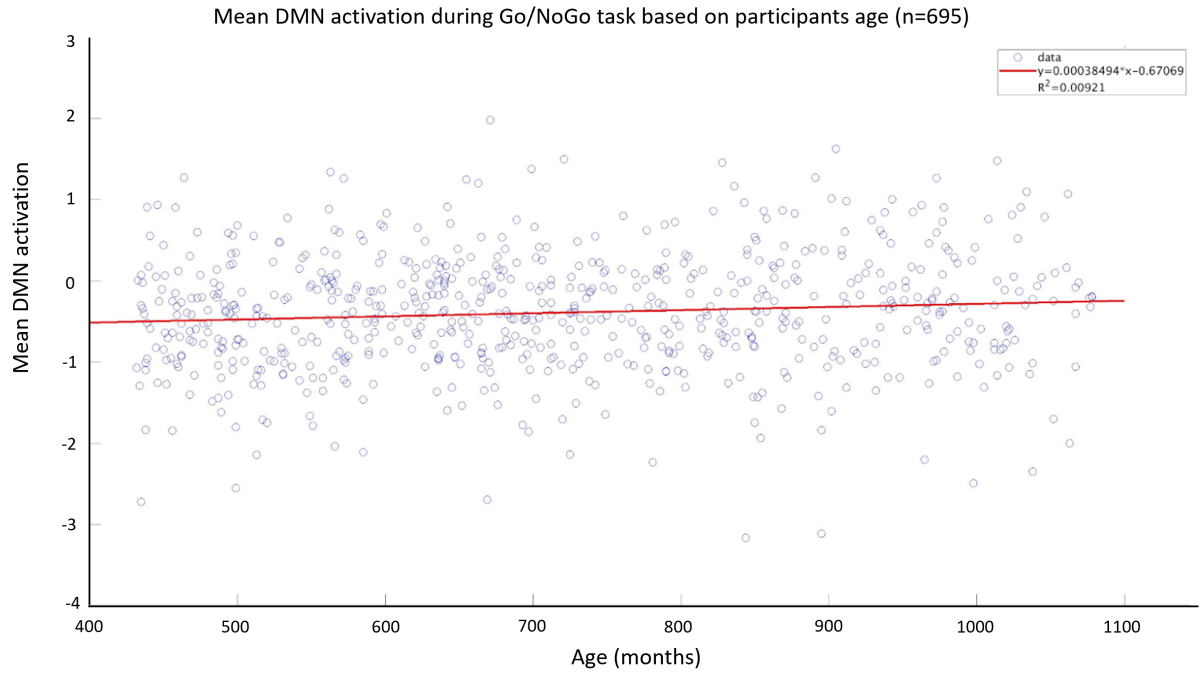

Figure 4.12: Graphing each participant's age (x-axis) and their mean DMN measurement during the task (y-axis). Linear regression model in red and its accompanying R-squared value.

4.6 DMN levels prior to NoGo trial response

On average, individuals with at least 3 incorrect NoGo responses (n=136) by pushing a button when asked to omit a button press, tended to have higher DMN levels prior to an incorrect response than prior to a correct response. There were notably significant differences between the two activation states 1.6 seconds to 5.6 seconds before a response as shown in Figure 4.13. Figure 4.14 reveals the p-values that fall below the Bonferroni correction of 0.005. Figure 4.15 reveals the most significant difference occurred 4.8 seconds prior to the stimulus being presented (p-value: 5.4896e-5). The age of participants who answered at least 3 NoGo trials incorrectly was evenly distributed. The mean was calculated at 794.3817 months, or 66.2 years, (σ=210.8220 months), the oldest individual was 1200 months old (100 years), and the youngest was 447 months (37.25 years). 68 of the 135 participants with ages reported were under 800 months (66.67 years) old and 63 were equal to or over this age.

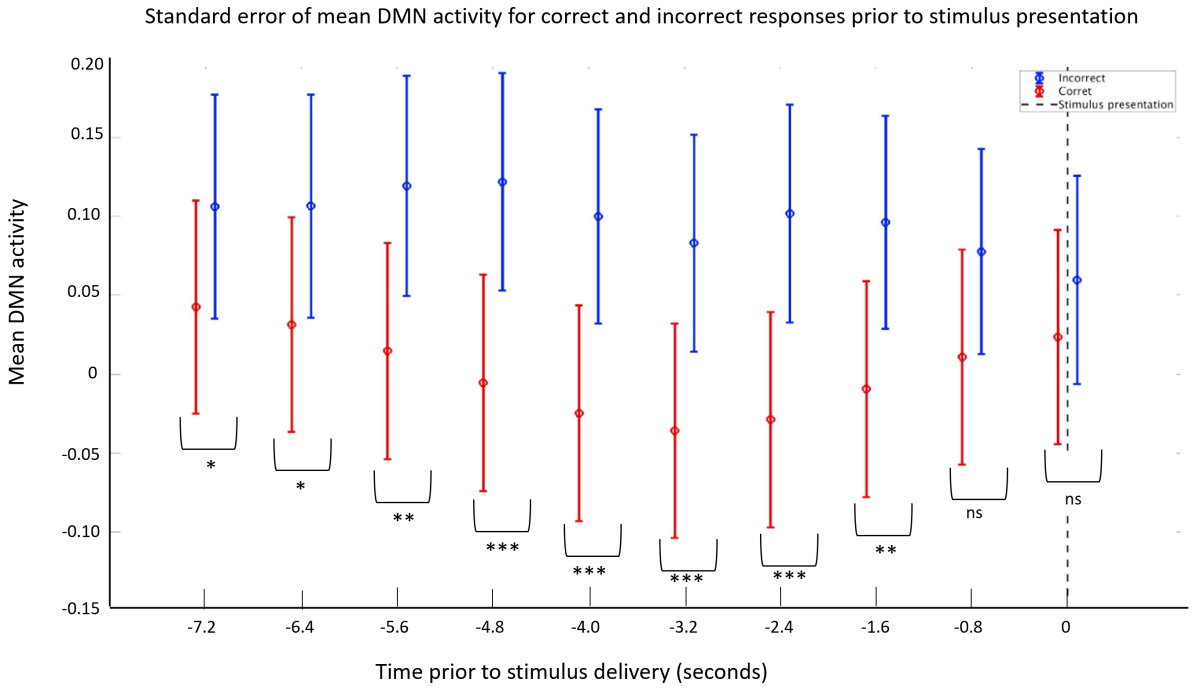

Figure 4.13: Mean DMN measurement of 136 subjects during and prior to a correct (red) or incorrect (blue) button omission for NoGo stimuli. Vertical dashed line indicates when the stimulus was presented. X-axis indicates how far back, in seconds, the DMN is being examined before the trial occurred. * represents when $P<0.05$, ** indicates when $P<0.01$, *** is used when $P<0.001$.

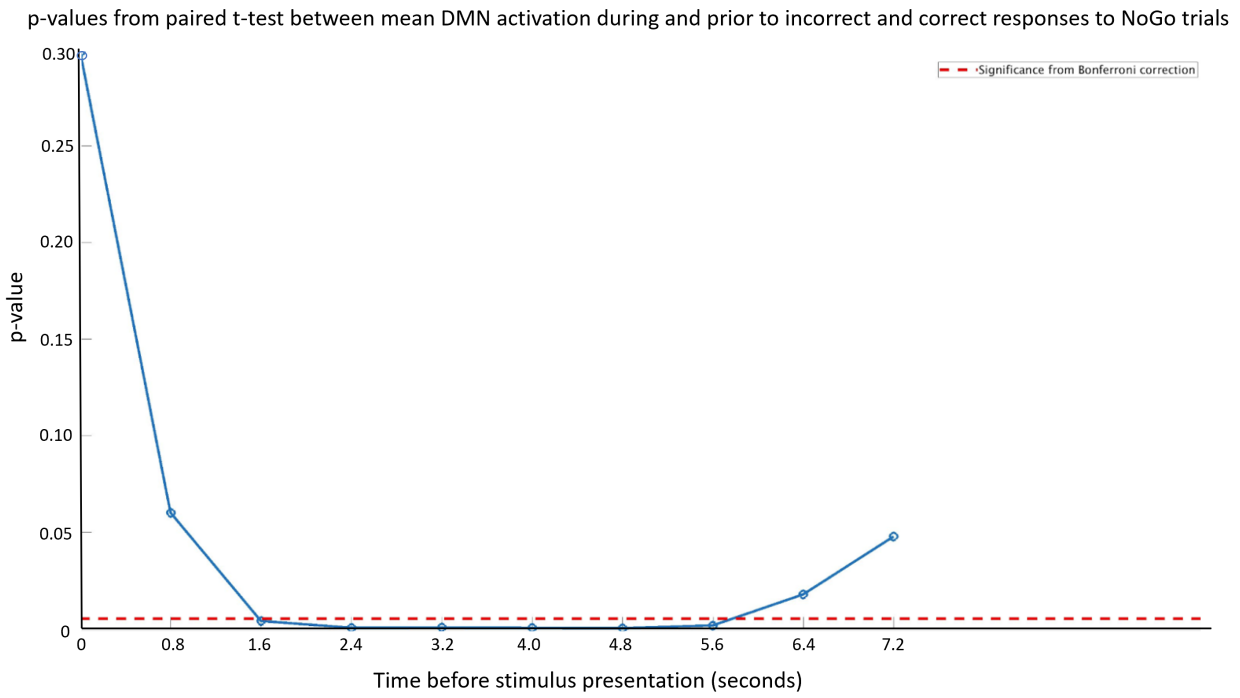

Figure 4.14: P-values calculated from a paired t-test between the mean DMN levels measured prior to correct and incorrect responses. Red horizontal line indicates a cutoff of significance based on Bonferroni correction (α=0.005).

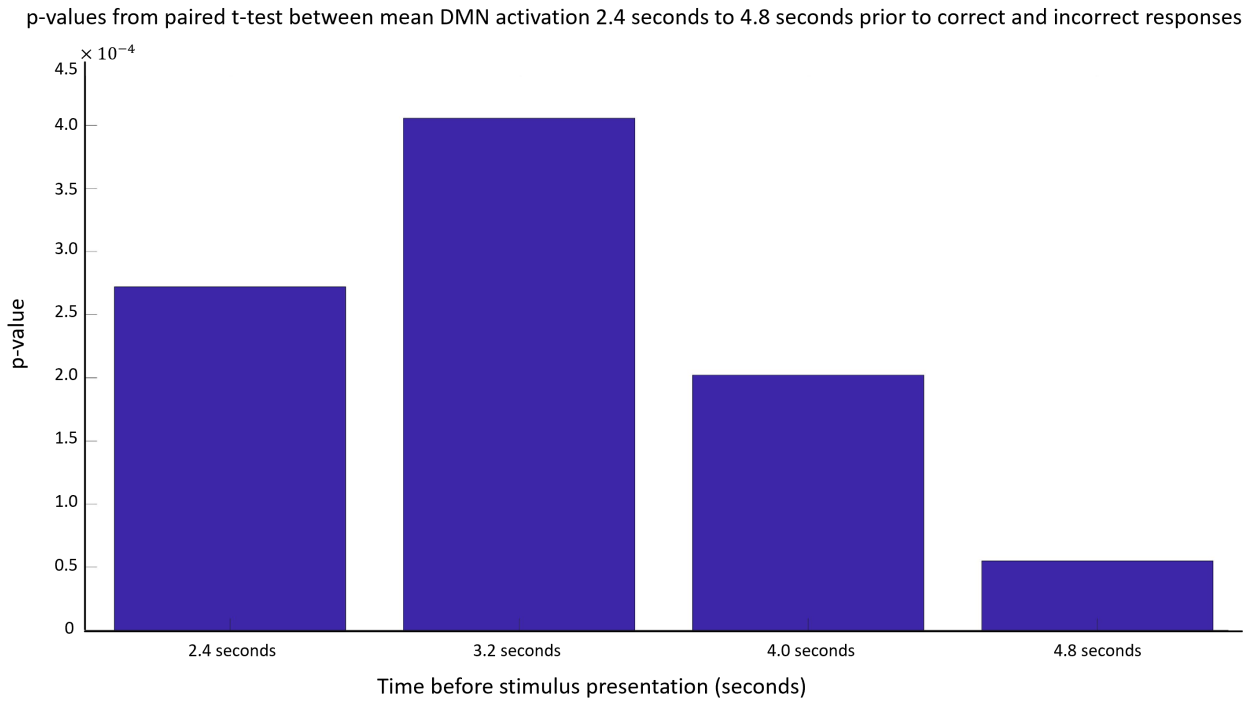

Figure 4.15: P-values calculated from a paired t-test between the mean DMN levels measured prior to correct and incorrect responses 2.4 seconds to 4.8 seconds before stimulus presentation.

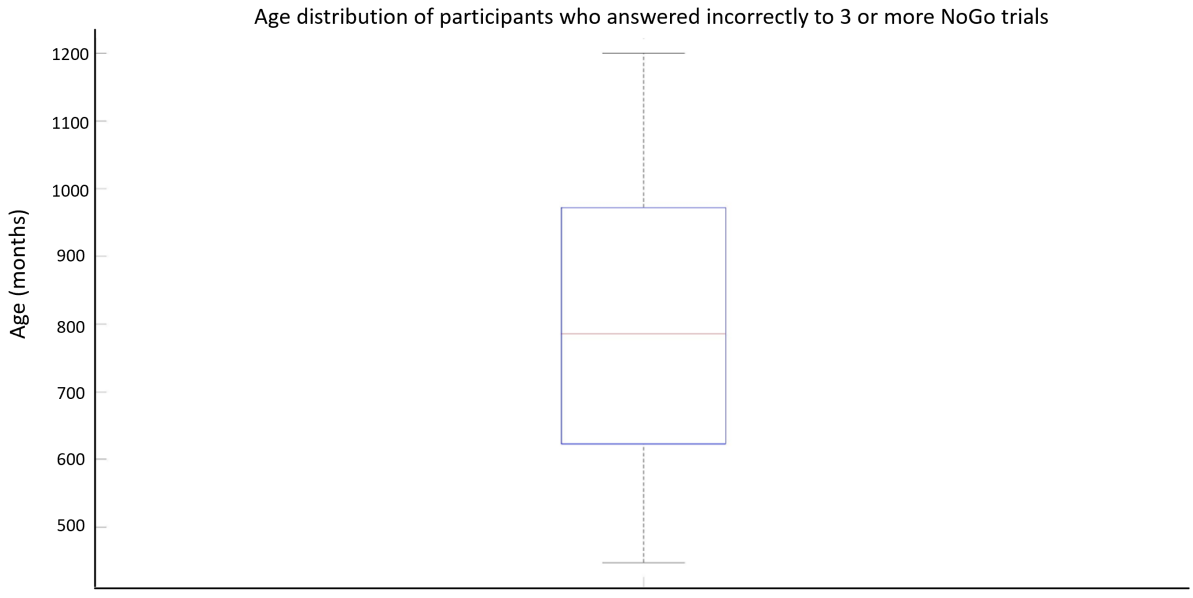

Figure 4.16: Age distribution for participants who answered at least 3 NoGo trials incorrectly.

4.7 Resting state DMN levels and task DMN levels

There were different distributional effects occurring in the DMN activation levels when at rest and during a task. The resting state distribution was standard normal (μ=-0.0014, σ=1.0827, κ=3.1884, γ=0.0768). Neither expressed skewness, however there was a shift to the left for the task distribution, blue histogram in Figure 4.17, with a mean of -0.3962. Furthermore a kurtosis level of 3.5002 and the higher peak in the task distribution revealed higher data collection around the mean.

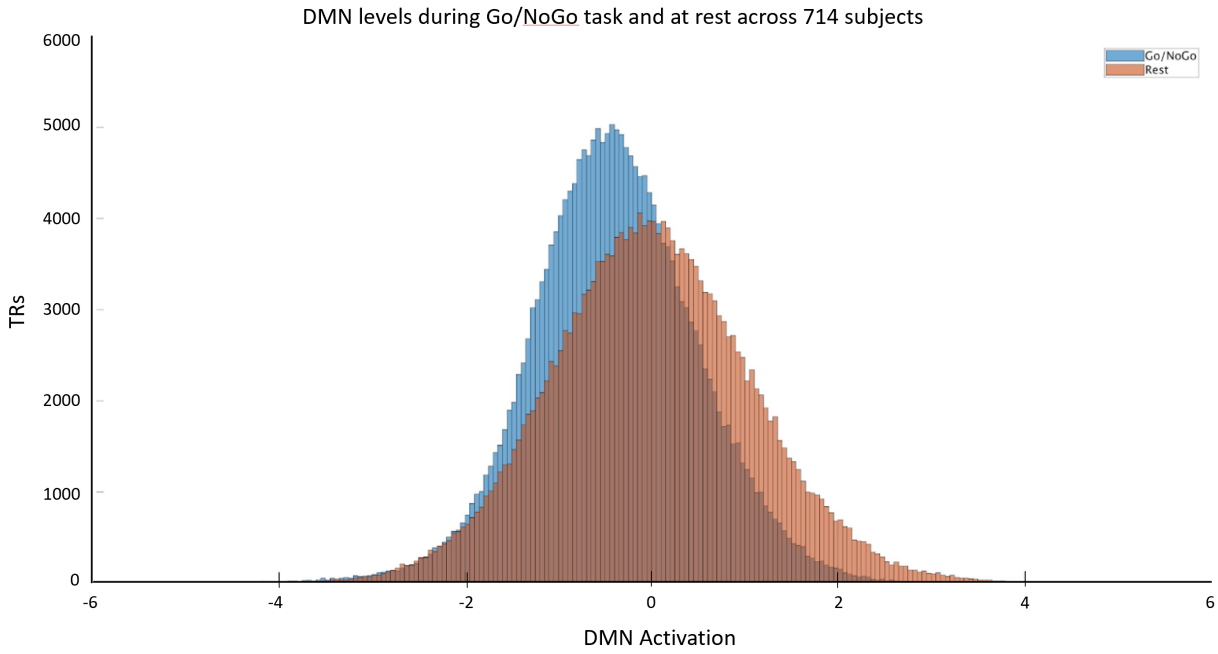

Figure 4.17: Distribution of all DMN levels collected in 714 subjects during a Go/NoGo task (blue) and during a resting state scan (orange-red).

4.8 Reaction time (RT) in Go trials

Results varied when comparing the mean DMN levels prior to Go response in 5 different RT ranges. Average DMN levels were reported to be higher before Go responses with particular reaction times across 711 subjects compared with 135 participants with frequent incorrect NoGo responses. This occurred in instances where RT≤0.2 seconds (Figure 4.18), 0.6<RT≤0.8s (Figure 4.21), and 0.8<RT (Figure 4.22). The inverse was reported for Go responses with 0.2s<RT≤0.4s (Figure 4.19), and 0.4s<RT≤0.6s (Figure 4.20).

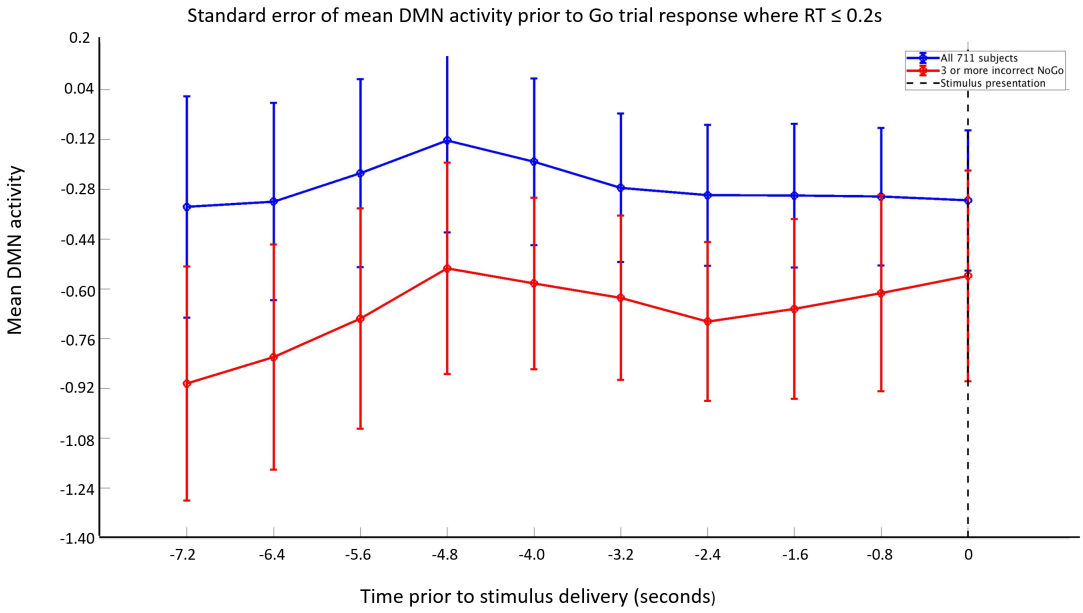

Figure 4.18: Mean DMN levels prior to Go trials with RT less than or equal to 0.2 seconds. Mean DMN levels at instances in participants that answered 3 or more NoGo trials incorrectly (red, n=7). Mean DMN levels at instances across all subjects (blue, n=12).

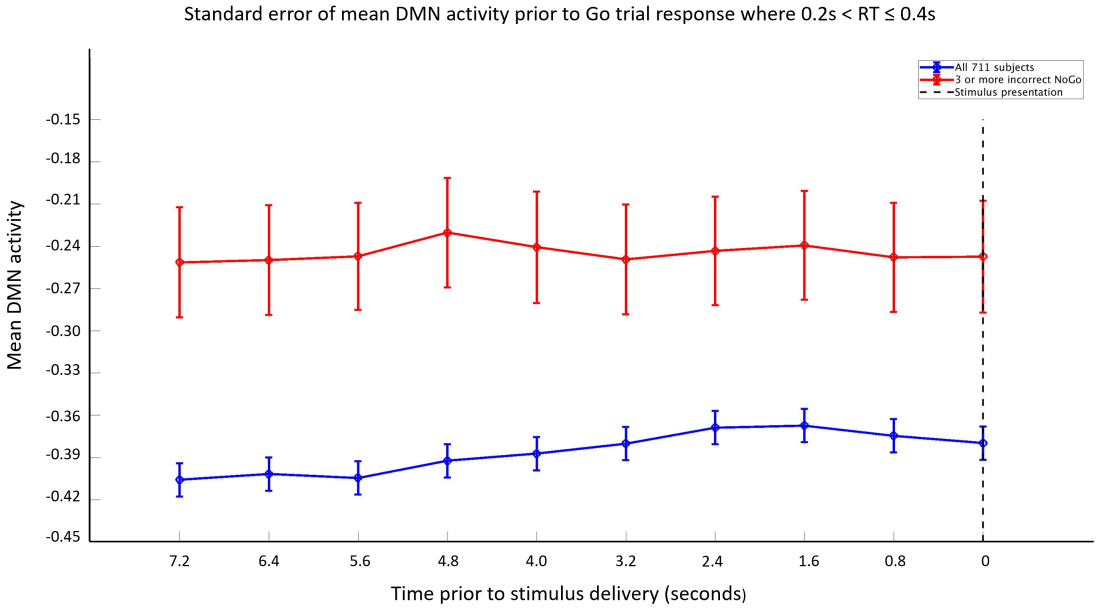

Figure 4.19: Mean DMN levels prior to Go trials with RT between 0.2 seconds and 0.4 seconds. Mean DMN levels at instances in participants that answered 3 or more NoGo trials incorrectly (red, n=575). Mean DMN levels at instances across all subjects (blue, n=5540).

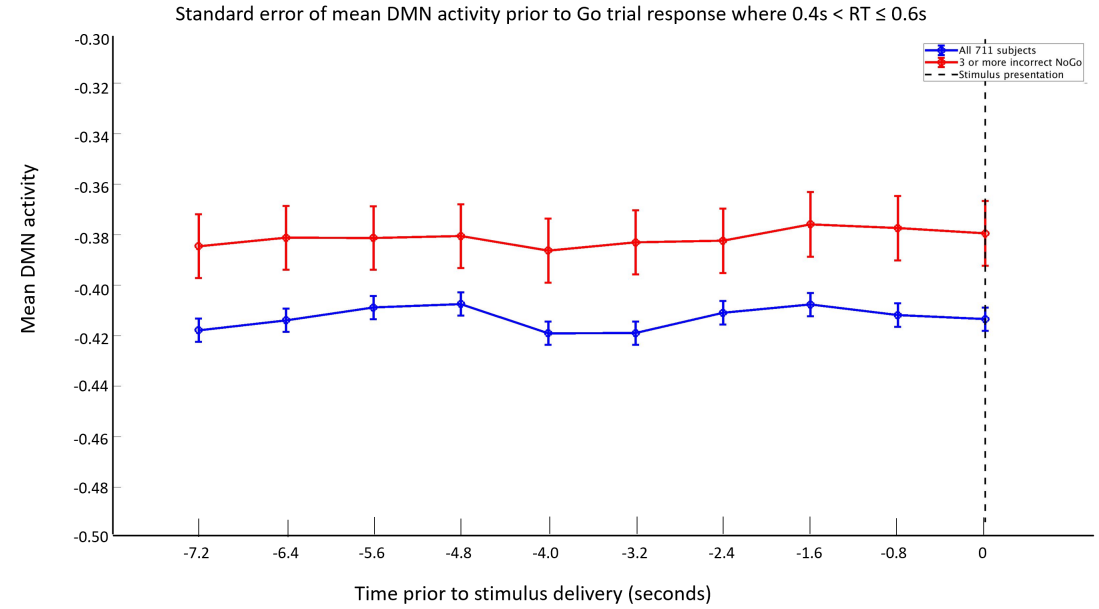

Figure 4.20: Mean DMN levels prior to Go trials with RT between 0.4 seconds and 0.6 seconds. Mean DMN levels at instances in participants that answered 3 or more NoGo trials incorrectly (red, n=4951). Mean DMN levels at instances across all subjects (blue, n=36245).

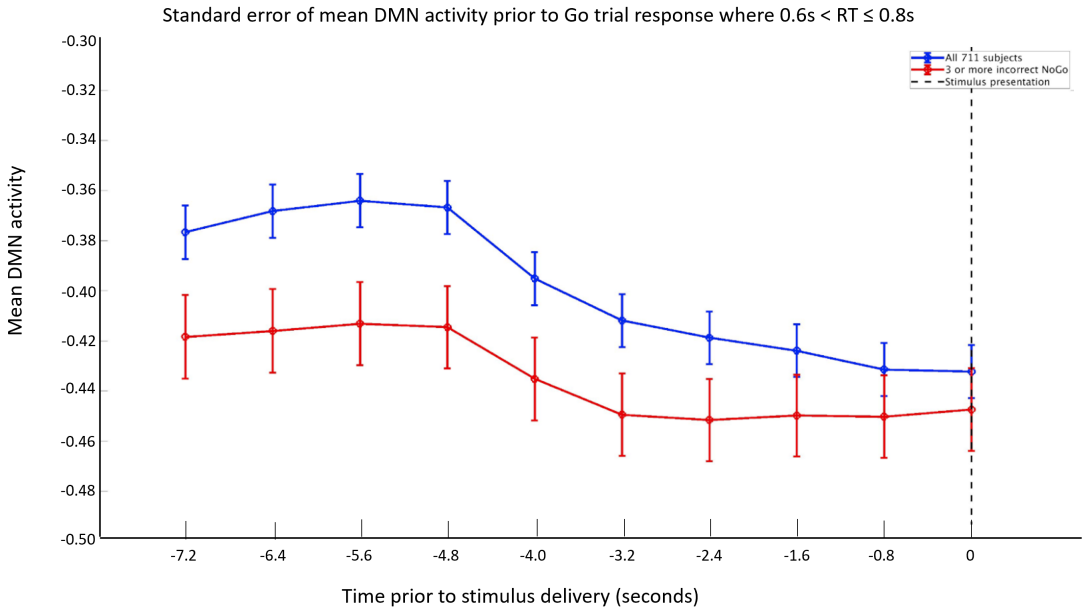

Figure 4.21: Mean DMN levels prior to Go trials with RT between 0.6 seconds and 0.8 seconds. Mean DMN levels at instances in participants that answered 3 or more NoGo trials incorrectly (red, n=2664). Mean DMN levels at instances across all subjects (blue, n=6878).

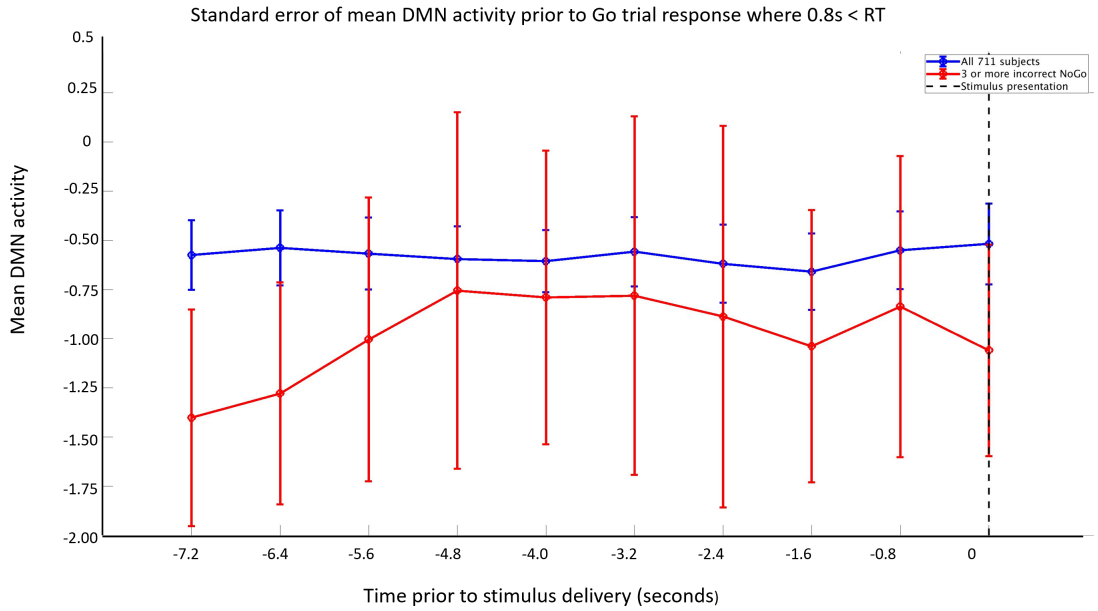

Figure 4.22: Mean DMN levels prior to Go trials with RT greater than 0.8 seconds. Mean DMN levels at instances in participants that answered 3 or more NoGo trials incorrectly (red, n=2). Mean DMN levels at instances across all subjects (blue, n=20).

Chapter 5

Discussion

The comparison between the open-loop and closed-loop simulations provided expected results as the latter performed at greater efficiency than its counterpart. The linear model demonstrated that while both methods could calculate the correct slope on average, there was a greater variance in answers across realizations. Controlling when data is collected through a closed-loop fMRI experiment provides greater precision in calculations. Additionally, as Figure 4.6 demonstrated, less participants would be required when performing this method and still provide adequately low margins of error. The number of subjects used in an open-looped event related experiment would need to be more than doubled to bring the margin of error down to the same level as a closed-loop design. Working with less subjects while maintaining accuracy benefits researchers in terms of compensation, time, and logistical paperwork. The same pattern also translated to the quadratic function simulation showing that the same idea holds regardless of the functional relationship we are trying to estimate. By purposefully selecting high and low DMN levels located at the tails of a distribution, variation in the network's functional role during tasks can be reduced and a fuller picture of its responsibilities be obtained.

The various distributions of DMN levels during a task were revealed to be leptokurtic with higher peaks located at their means. This supported the hypothesis that open-looped fMRI experiments oversample at the means and undersample the tails. Resting state scans of the DMN from the WashU and HCP-A data sets produced normal distributions. Additionally,

every distribution of DMN levels from a task were shifted to the left and had mean values around -0.4. By simply performing a task, it can be expected that the DMN will generally be more deactivated. This could be that subjects enter a more focused mindset before undergoing the task in order to perform better. This shift must be accounted for when designing a closed-loop experiment that delivers a stimulus when DMN levels pass a certain threshold. When comparing the two distributions in Figure 4.17, DMN activation levels are lower at the tails when performing a task. This will require the threshold in a closed-loop study to be lowered to adjust for this shift. Interestingly, the shift in deactivation on average was not related to the participant's age.

Differences were reported in the mean DMN levels prior to a correct NoGo response and an incorrect reply. This was expected as there have been similar findings reported in other studies [5, 10, 11, 19, 24, 34]. Surprisingly, there did not appear to be a correlation between these findings and age. Figure 4.16 supports that individuals could perform poorly on the NoGo tasks despite their age, however the cutoff for insufficient execution was 3 or more incorrect replies. A further look could be taken to determine if older people had a greater number of incorrect responses than younger. This could imply that mind wandering becomes increasingly more common as you age, thus resulting in more mistakes to tasks that require focus.

Unexpectedly was the variation in mean DMN levels before Go responses based on the reaction time to the trial. There were instances where clear differences could be observed, Figures 4.19, 4.20 and 4.21, while others were more unclear. This could be explained due to the differing population sizes, as seen in the total occurrences for RT greater than 0.8 seconds in subjects with three or more wrong NoGo responses (n=2). A larger data set could possibly reveal different trends however due to the size of the HCP-A study, this is most likely not feasible. More likely these variations could be explained by looking at the RT variability in subjects as was performed by Esterman et al. [11]. In this study, researchers

found differences in DMN levels when subjects had higher RT variability compared to lower RT variability. Future studies with this data set could reveal similar outcomes through RT variability rather than solely based on the speed of the button press for a Go trial. Additionally, the age was not explored based on RT. It would be expected that RT would be slower for older subjects, due to reductions in motor function. Exploring age and RT variability between Go trials in each subject would remove impaired motor function as a variable to button pressing speed and base performance on DMN levels. In turn this could reveal possible changes in DMN activity as one ages.

Chapter 6

Conclusions

The purpose of this study was to support innovation in closed-loop fMRI studies by building simulations and studying DMN activation during open-loop task experiments. It was hypothesized that data collection simulating an open-loop design would be less efficient than that of a closed-loop simulation. When comparing the two methods, an open-loop simulation produced higher margins of error and greater variation than a closed-loop design. It was also expected that when observing DMN levels collected during an open-loop experiment there would be oversampling at the mean DMN levels. DMN distributions recorded during a Go/NoGo task revealed this to be true. Additionally, task distributions revealed minor suppression in the DMN on average with a value around -0.4. This pattern was not observed when plotting resting state DMN levels, as it was shown to be normally distributed. Finally, DMN levels differed based on response to a NoGo trial and between those prone to mistakes during these tasks. DMN levels were higher during and prior to incorrect NoGo responses, with heightened significance occurring 1.6 seconds to 5.6 seconds before stimulus presentation. Individual's that had 3 or more incorrect NoGo responses also had higher DMN levels on average during Go trials with certain reaction times. This was reported for reaction times between 0.2 and 0.4 seconds and between 0.4 and 0.6 seconds. In situations where reaction times were faster than 0.2 seconds, between 0.6 and 0.8 seconds, and longer than 0.8 seconds, these same individual's showed lower mean DMN levels than the entire subject population in the HCP-A study. From the findings, it is beneficial to utilize a closed-loop

design as it reduces variation and margins of error in results and will limit under sampling of data located at the tails of the distribution. When designing a closed-loop study, minor suppression in DMN levels during a task must be accounted for when setting thresholds for delivering stimulus based on recorded brain levels. Additionally, understanding trends in a DMN level time series based on responses to tasks can help determine when a stimulus can be presented to capture a desired result (i.e. correct or incorrect response).

This project was successful in creating statistical arguments for closed-loop studies. It was shown through simulations that greater control over data collection at high and low activation states was superior to the random nature of an open-loop procedure. Statistical differences between correct and incorrect responses during NoGo trials and at varying reaction times for Go experiments were observed in the DMN. Variations in mean DMN levels depending on RT to Go trials were reported between individuals more prone to incorrect NoGo tasks and all subjects. Additional research into the RT variation between trials may provide clearer explanations to this event. Distributional effects in the DMN across multiple participants revealed suppression on average and greater peaks at the mean while performing a task. This general shift towards suppression must be accounted for when designing future real time ER-fMRI experiments, for greater efficiency at sampling at the tails. It is the hope that the statistical arguments presented in this study reinforce future development of more statistically powerful closed-loop experiments.

Bibliography

[1] Connectome programs, Jun 2022. URL https://neuroscienceblueprint.nih.gov/human-connectome/connectome-programs#:~:text=Launched%20in%202009%20as%20a,connectivity%20of%20the%20human%20brain.

[2] John T Arsenault, Natalie Caspari, Rik Vandenberghe, and Wim Vanduffel. Attention shifts recruit the monkey default mode network. *Journal of Neuroscience*, 38(5):1202–1217, 2018.

[3] Anita D Barber, Brian S Caffo, James J Pekar, and Stewart H Mostofsky. Decoupling of reaction time-related default mode network activity with cognitive demand. *Brain imaging and behavior*, 11(3):666–676, 2017.

[4] Deanna M Barch, Gregory C Burgess, Michael P Harms, Steven E Petersen, Bradley L Schlaggar, Maurizio Corbetta, Matthew F Glasser, Sandra Curtiss, Sachin Dixit, Cindy Feldt, et al. Function in the human connectome: task-fmri and individual differences in behavior. *Neuroimage*, 80:169–189, 2013.

[5] Mélanie Boly, Evelyne Balteau, Caroline Schnakers, Christian Degueldre, Gustave Moonen, André Luxen, Christophe Phillips, Philippe Peigneux, Pierre Maquet, and Steven Laureys. Baseline brain activity fluctuations predict somatosensory perception in humans. *Proceedings of the National Academy of Sciences*, 104(29):12187–12192, 2007.

[6] Susan Y Bookheimer, David H Salat, Melissa Terpstra, Beau M Ances, Deanna M Barch, Randy L Buckner, Gregory C Burgess, Sandra W Curtiss, Mirella Diaz-Santos, Jennifer Stine Elam, et al. The lifespan human connectome project in aging: an overview. *Neuroimage*, 185:335–348, 2019.

[7] Megan T Debettencourt, Jonathan D Cohen, Ray F Lee, Kenneth A Norman, and Nicholas B Turk-Browne. Closed-loop training of attention with real-time brain imaging. *Nature neuroscience*, 18(3):470–475, 2015.

[8] Matthew L Dixon, Alejandro De La Vega, Caitlin Mills, Jessica Andrews-Hanna, R Nathan Spreng, Michael W Cole, and Kalina Christoff. "heterogeneity within the frontoparietal control network and its relationship to the default and dorsal attention networks": Correction. 2018.

[9] Nico UF Dosenbach, Damien A Fair, Francis M Miezin, Alexander L Cohen, Kristin K Wenger, Ronny AT Dosenbach, Michael D Fox, Abraham Z Snyder, Justin L Vincent, Marcus E Raichle, et al. Distinct brain networks for adaptive and stable task control in humans. *Proceedings of the National Academy of Sciences*, 104(26):11073–11078, 2007.

[10] Tom Eichele, Stefan Debener, Vince D Calhoun, Karsten Specht, Andreas K Engel, Kenneth Hugdahl, D Yves Von Cramon, and Markus Ullsperger. Prediction of human errors by maladaptive changes in event-related brain networks. *Proceedings of the National Academy of Sciences*, 105(16):6173–6178, 2008.

[11] Michael Esterman, Sarah K Noonan, Monica Rosenberg, and Joseph DeGutis. In the zone or zoning out? tracking behavioral and neural fluctuations during sustained attention. *Cerebral cortex*, 23(11):2712–2723, 2013.

[12] Flavio Frohlich and Leah Townsend. Closed-loop transcranial alternating current stimulation: towards personalized non-invasive brain stimulation for the treatment of psychiatric illnesses. *Current Behavioral Neuroscience Reports*, 8:51–57, 2021.

[13] Kathleen A Garrison, Dustin Scheinost, Patrick D Worhunsky, Hani M Elwafi, Thomas A Thornhill IV, Evan Thompson, Clifford Saron, Gaelle Desbordes, Hedy

Kober, Michelle Hampson, et al. Real-time fmri links subjective experience with brain activity during focused attention. *Neuroimage*, 81:110–118, 2013.

[14] Oyetunde Gbadeyan, James Teng, and Ruchika Shaurya Prakash. Predicting response time variability from task and resting-state functional connectivity in the aging brain. *NeuroImage*, 250:118890, 2022.

[15] Meher R Juttukonda, Binyin Li, Randa Almaktoum, Kimberly A Stephens, Kathryn M Yochim, Essa Yacoub, Randy L Buckner, and David H Salat. Characterizing cerebral hemodynamics across the adult lifespan with arterial spin labeling mri data from the human connectome project-aging. *Neuroimage*, 230:117807, 2021.

[16] Mayuresh S Korgaonkar, Stuart M Grieve, Amit Etkin, Stephen H Koslow, and Leanne M Williams. Using standardized fmri protocols to identify patterns of prefrontal circuit dysregulation that are common and specific to cognitive and emotional tasks in major depressive disorder: first wave results from the ispot-d study. *Neuropsychopharmacology*, 38(5):863–871, 2013.

[17] Robert Langner, Thilo Kellermann, Simon B Eickhoff, Frank Boers, Anjan Chatterjee, Klaus Willmes, and Walter Sturm. Staying responsive to the world: Modality-specific and-nonspecific contributions to speeded auditory, tactile, and visual stimulus detection. *Human brain mapping*, 33(2):398–418, 2012.

[18] Binyin Li, Ikbeom Jang, Joost Riphagen, Randa Almaktoum, Kathryn Morrison Yochim, Beau M Ances, Susan Y Bookheimer, David H Salat, and Alzheimer's Disease Neuroimaging Initiative. Identifying individuals with alzheimer's disease-like brains based on structural imaging in the human connectome project aging cohort. *Human brain mapping*, 42(17):5535–5546, 2021.

[19] Chiang-Shan Ray Li, Peisi Yan, Keri L Bergquist, and Rajita Sinha. Greater activation of the "default" brain regions predicts stop signal errors. *Neuroimage*, 38(3):640–648, 2007.

[20] Amalia R McDonald, Jordan Muraskin, Nicholas T Van Dam, Caroline Froehlich, Benjamin Puccio, John Pellman, Clemens CC Bauer, Alexis Akeyson, Melissa M Breland, Vince D Calhoun, et al. The real-time fmri neurofeedback based stratification of default network regulation neuroimaging data repository. *NeuroImage*, 146:157–170, 2017.

[21] Jyoti Mishra and Adam Gazzaley. Closed-loop rehabilitation of age-related cognitive disorders. In *Seminars in neurology*, volume 34, pages 584–590. Thieme Medical Publishers, 2014.

[22] Krishna P Miyapuram. Introduction to fmri: experimental design and data analysis. 2008.

[23] Neil L Nixon, Peter F Liddle, Graham Worwood, M Liotti, and E Nixon. Prefrontal cortex function in remitted major depressive disorder. *Psychological Medicine*, 43(6): 1219–1230, 2013.

[24] Giuseppe Pagnoni. Dynamical properties of bold activity from the ventral posteromedial cortex associated with meditation and attentional skills. *Journal of Neuroscience*, 32 (15):5242–5249, 2012.

[25] Maria Chiara Piani, Eleonora Maggioni, Giuseppe Delvecchio, and Paolo Brambilla. Sustained attention alterations in major depressive disorder: A review of fmri studies employing go/no-go and cpt tasks. *Journal of Affective Disorders*, 2022.

[26] Jonathan D Power, Anish Mitra, Timothy O Laumann, Abraham Z Snyder, Bradley L

Schlaggar, and Steven E Petersen. Methods to detect, characterize, and remove motion artifact in resting state fmri. *Neuroimage*, 84:320–341, 2014.

[27] Marcus E Raichle. The brain's default mode network. *Annual review of neuroscience*, 38:433–447, 2015.

[28] Sepideh Sadaghiani, Guido Hesselmann, and Andreas Kleinschmidt. Distributed and antagonistic contributions of ongoing activity fluctuations to auditory stimulus detection. *Journal of Neuroscience*, 29(42):13410–13417, 2009.

[29] Ashish K Sahib, Joana RA Loureiro, Megha M Vasavada, Antoni Kubicki, Benjamin Wade, Shantanu H Joshi, Roger P Woods, Eliza Congdon, Randall Espinoza, and Katherine L Narr. Modulation of inhibitory control networks relate to clinical response following ketamine therapy in major depression. *Translational psychiatry*, 10(1):260, 2020.

[30] Kazuhisa Shibata, Takeo Watanabe, Yuka Sasaki, and Mitsuo Kawato. Perceptual learning incepted by decoded fmri neurofeedback without stimulus presentation. *science*, 334(6061):1413–1415, 2011.

[31] Lin Sørensen, Yu Sun Chung, Sabin Khadka, and Michael C Stevens. Moment-to-moment fluctuations of hemodynamic responses in posterior default mode networks differentially predict level of attentional lapses in adolescents with attention-deficit/hyperactivity disorder. *medRxiv*, pages 2022–01, 2022.

[32] UpAndRunning. Components of the human connectome project - task fmri - connectome. URL https://www.humanconnectome.org/study/hcp-young-adult/project-protocol/task-fmri#:~:text=These%20%E2%80%9Cfunctional%20localizer%E2%80%9D%20tasks%20include,processing%2C%20and%20decision%2Dmaking.

[33] Tor D Wager and Thomas E Nichols. Optimization of experimental design in fmri: a general framework using a genetic algorithm. *Neuroimage*, 18(2):293–309, 2003.

[34] Daniel H Weissman, KC Roberts, KM Visscher, and MG Woldorff. The neural bases of momentary lapses in attention. *Nature neuroscience*, 9(7):971–978, 2006.

[35] Nikolaus Wenger, Eduardo Martin Moraud, Stanisa Raspopovic, Marco Bonizzato, Jack DiGiovanna, Pavel Musienko, Manfred Morari, Silvestro Micera, and Grégoire Courtine. Closed-loop neuromodulation of spinal sensorimotor circuits controls refined locomotion after complete spinal cord injury. *Science translational medicine*, 6(255):255ra133–255ra133, 2014.

[36] Stavros Zanos. Closed-loop neuromodulation in physiological and translational research. *Cold Spring Harbor perspectives in medicine*, 9(11):a034314, 2019.

Appendices

Appendix A

First Appendix

A.1 Section one

Confidence Interval (CI):

$$CI = \mu \pm Z * \frac{\sigma}{\sqrt{n}}$$

μ=mean of population

Z=z-score based on % confidence (z=1.96 for 95% confidence)

σ=standard deviation of population

n=population size

Margin of Error (ME):

$$ME = Z * \frac{\sigma}{\sqrt{n}}$$

Z=z-score based on % confidence (z=1.96 for 95% confidence)

σ=standard deviation of population

n=population size

Appendix B

Second Appendix

Optseq2 parameters (explained in https://surfer.nmr.mgh.harvard.edu/optseq/optseq2.help.txt):

Number of time points per schedule (ntp)= 296

Time between stimuli (tr)= 1.25 seconds

Window of time for participant to respond (psdwin)= 0-2.5 seconds

Minimum amount of time between null stimulus and event stimuli (tnullmin)= 0 seconds

Maximum amount of time for null stimulus (tnullmax)= 20 seconds

Event 1 occurring 48 times and lasting 1.25 seconds each (ev evt1 1.25 48)

Event 2 occurring 48 times and lasting 1.25 seconds each (ev evt2 1.25 48)

Save 120 files for each participant (nkeep 120)

Search most optimal times from 10000 outcomes (nsearch 10000)